EFFECT OF RIB SPACING ON HEAT TRANSFER AND FRICTION IN A ROTATING TWO-PASS RECTANGULAR (AR=1:2) CHANNEL

A Thesis

by

YAO-HSIEN LIU

Submitted to the Office of Graduate Studies of
Texas A&M University
in partial fulfillment of the requirements for the degree of

MASTER OF SCIENCE

August 2005

Major Subject: Mechanical Engineering

EFFECT OF RIB SPACING ON HEAT TRANSFER AND FRICTION IN A ROTATING TWO-PASS RECTANGULAR (AR=1:2) CHANNEL

A Thesis

by

YAO-HSIEN LIU

Submitted to the Office of Graduate Studies of
Texas A&M University
in partial fulfillment of the requirements for the degree of

MASTER OF SCIENCE

Approved by:

Chair of Committee,	Je-Chin Han
Committee Members,	N. K. Anand
	Hamn-Ching Chen
Head of Department,	Dennis O'Neal

August 2005

Major Subject: Mechanical Engineering

ABSTRACT

Effect of Rib Spacing on Heat Transfer and Friction in a Rotating Two-Pass Rectangular (AR=1:2) Channel. (August 2005)

Yao-Hsien Liu, B.S., National Taiwan University

Chair of Advisory Committee: Dr. Je-Chin Han

The research focuses on testing the heat transfer enhancement in a channel for different spacing of the rib turbulators. Those ribs are put on the surface in the two pass rectangular channel with an aspect ratio of AR=1:2. The cross section of the rib is 1.59 x 1.59 mm. Those ribs are put on the leading and trailing walls of the channel with the angle of flow attack to the mainstream of 45°. The rotating speed is fixed at 550-RPM with the channel orientation at β=90°. Air is used as the coolant through the cooling passage with the coolant-to-wall density ratio ($\Delta\rho/\rho$) maintained around 0.115 in the first pass and 0.08 in the second pass. The Reynolds numbers are controlled at 5000, 10000, 25000, and 40000. The rib spacing-to-height ratios (P/e) are 3, 5, 7.5, and 10. The heat transfer coefficient and friction factor are measured to determine the effect of the different rib distributions. Stationary cases and rotational cases are examined and compared. The result shows that the highest thermal performance is P/e=5 for the stationary case and P/e=7.5 for the rotating case.

DEDICATION

To my parents and sister for their endless love, support and encouragement.

ACKNOWLEDGEMENTS

I am very grateful to Dr. J. C. Han for giving me the opportunity to do research in the area of turbine heat transfer technology. He has provided me valuable experience in this area through his teaching and research. I am appreciative that Dr. N. K. Anand and Dr. H. C. Chen have served on my committee and gave me suggestions on my research and thesis. I also thank the experienced partners in the lab who always gave me helpful advice and solutions.

TABLE OF CONTENTS

Page

Page

LIST OF FIGURES

FIGURE Page

LIST OF TABLES

NOMENCLATURE

A_{smooth}	smooth area of the copper plate
A_{total}	total area of the copper plate and the rib
AR	channel aspect ratio, W/H
AR_{rib}	rib aspect ratio, e/w
Bo_x	buoyancy parameter, $(\Delta\rho/\rho)_x Ro^2 (R_x/D_h)$
D_h	hydraulic diameter
e	rib height
f	friction factor
f_0	fully-developed friction factor in non-rotating smooth tube
H	channel height
h	local heat transfer coefficient
k	thermal conductivity of the coolant ($W/m \cdot K$)
L	length of the rib-roughened portion of the test secion
Nu	local Nusselt number, hD_h/k
Nu_0	Nusselt number of the fully-developed turbulent flow in smooth pipe
P	rib pitch
P_i	pressure at the inlet of the test section
P_o	pressure at the outlet of the test section
Pr	Prandtl number

q''_{losst}	heat loss through the wall
q''_{w}	heat flux at the wall
Re	Reynolds number, $\rho V D_h / \mu$
Ro	Rotation number, $\Omega D_h / V$
T_w	wall temperature
T_b	local coolant bulk temperature
V	bulk velocity in streamwise direction
W	channel width
w	rib width
α	rib angle of attack
β	angle of the channel orientation with respect to the axis of rotation
μ	viscosity of the coolant
ρ	density of the coolant
$\left(\frac{\Delta\rho}{\rho}\right)_x$	inlet coolant-to-wall density ratio
Ω	rotation speed, RPM

INTRODUCTION

Gas turbine blade heat transfer and cooling technology has been studied to reduce the thermal load and to improve the heat transfer coefficient [1]. The cooling methods can help reduce the temperature of the blade and prevent it from being damaged by the high temperature. Turbine blade internal cooling technology involves sending coolant through the cooling channels inside the turbine blade. Figure 1 shows the cooling channels inside the gas turbine blade. Jet impingement cooling is used in the leading edge where the thermal load is excessively high. Pin-fin cooling is used in the trailing edge where the jet impingement and rib-roughened channel cannot be applied due to manufacturing constrains. The rib-roughened channel is applied in the middle portion of the turbine blade.

In order to increase the cooling efficiency, the cooling passage is roughened with ribs to trip the boundary layer and the flow will reattach to the surface which will increase the heat transfer coefficients. These ribs can also enhance the heat transfer by mixing the core coolant with the hot air near the wall and reduce the temperature of the turbine blade. However, the heat transfer enhancement comes at the expense of increased pressure losses. The rib distributions are an important issue for the internal cooling. Several parameters such as channel aspect ratio (AR), rib spacing to height ratio (P/e), and rib height to hydraulic diameter ratio (e/D_h) or the blockage ratio (e/H) are key factors that affect the heat transfer and the fluid flow.

This thesis follows the style of Journal of Turbomachinery.

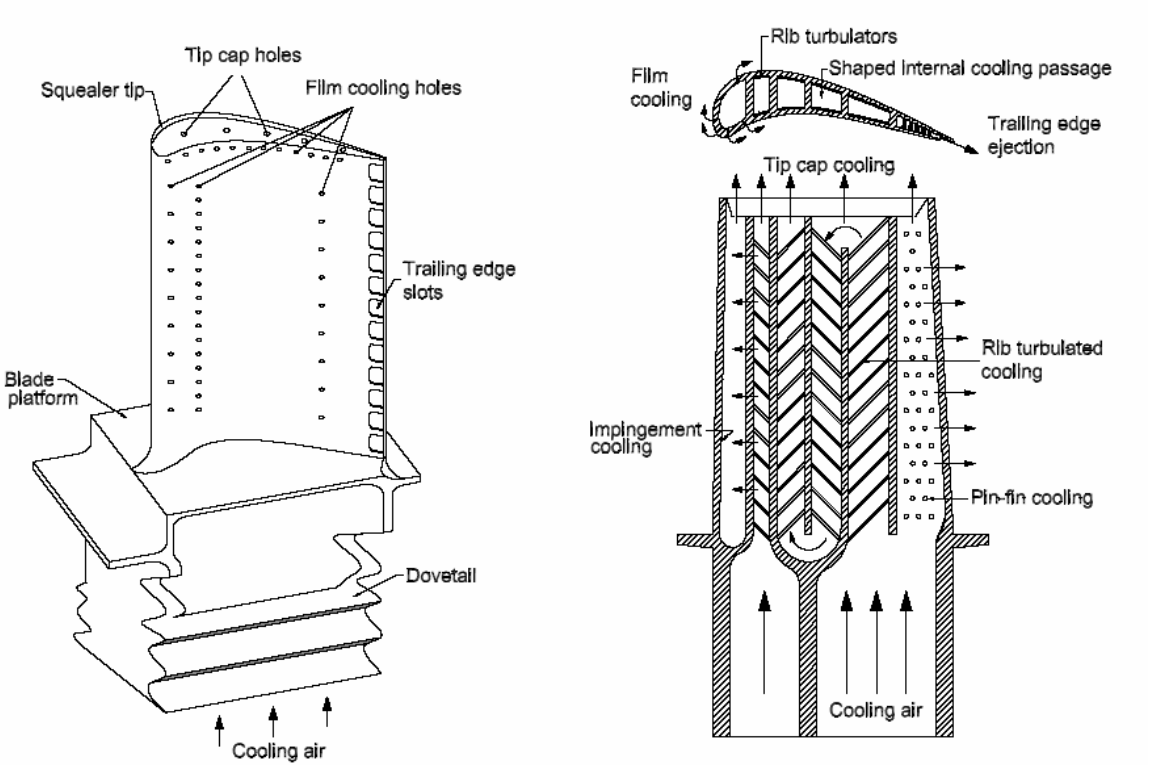

Fig. 1 Turbine Blade Cooling Technology [1]

Effect of Rib Spacing

The flow inside the rib-roughened channel will be tripped by the ribs and then reattach the surface. The spacing between the ribs will affect the flow reattachment. The reattachment effects will also decrease due to decreasing number of the ribs. Taslim and Lengkong [2] focused on the heat transfer coefficient and friction factor of the different spacing and the height of the 45° staggered square ribs in the square channel. The rib spacing-to-height ratios are 5, 8.5 and 10 and the height-to-passage hydraulic diameter ratios are 0.133, 0.167 and 0.25. They concluded that the spacing-to-height ratio equal to 5 would result in the highest heat transfer coefficient for the high blockage 45° angled ribs. But for the low blockage ribs the heat transfer coefficients are very close to each other. Taslim and Korotky [3] tested the low-aspect-ratio (AR_{rib} = 0.667) ribs in the square channel with an angle of attack of 90°. The P/e ratios of those ribs are 5, 8.5 and 10 and the height-to-passage hydraulic diameter ratios are 0.133, 0.167 and 0.25. The heat transfer coefficients and friction factors are compared with the results of the square ribs. Han [4] studied the fully developed turbulent flow in the square ducts with two opposite rib-roughened walls. He tested the heat transfer coefficient and friction factor with the P/e ratio of 10, 20 and 40 under the Reynolds numbers of 7000 to 90000. He found that both the friction factors and the Stanton number factors decrease with the increasing P/e ratio. Taslim and Spring [5] used liquid crystal to investigate the effects of turbulator profile and spacing on the heat transfer coefficient. The results show that the turbulators with aspect ratios (AR_{rib}) greater than unity produce higher heat transfer

coefficients at the expense of higher pressure losses. They tested 90° angled ribs in the staggered arrangement. Han [6] investigated two rib spacings (P/e=10 and 20) in the rectangular channel with channel aspect ratios of 1/4, 1/2, 1, 2 and 4. The results show that the Nusselt number ratios are the same trend on the ribbed side and the smooth side walls for different channel aspect ratios. But the local Nusselt number ratios in larger aspect ratio channels (W/H = 2 or 4) are higher than those in the smaller aspect ratio channels (W/H = 1/2 or 1/4). Han et al. [7] examined the heat transfer and friction for the rib-roughened surface under different P/e, e/D_h, e/w, and angle of flow attack. The ribs at 45° angle of flow attack were found to have superior thermal performance than those ribs at 90° angle of attack. They tested P/e ratio from 5 to 20. They found that the Stanton number at about P/e ratio of 10 is larger than of 5 at 90° angle of attack.

The secondary flow induced by the 90° angled ribs can be seen in Figure 2. The flow will not reattach to the surface if the spacing is too small between the ribs. On the other hand, the flow will create a boundary layer after reattachment if the spacing is too large. The flow reattachment effects will diminish due to the decreasing spacing between the ribs. But for the 45° angled ribs, the secondary flow is created and deflected by the ribs which can be seen in Figure 3. The flow will be deflected by the ribs and result in a different flow pattern compared to the 90° ribs. Taslim and Lengkong [2] also provide data to show that the heat transfer coefficient of the 45° rib is higher than 90° rib for the different spacing between the ribs.

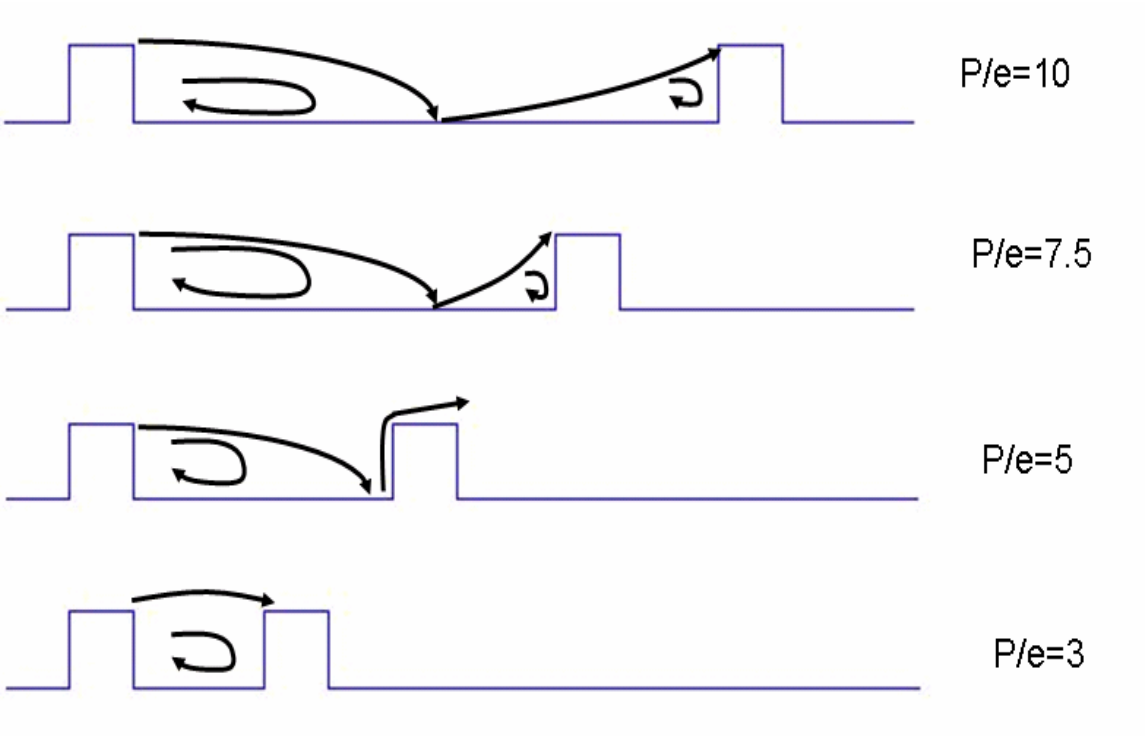

Fig. 2 The Flow Tripped by the Ribs and the Reattachment for the 90° Angled Ribs

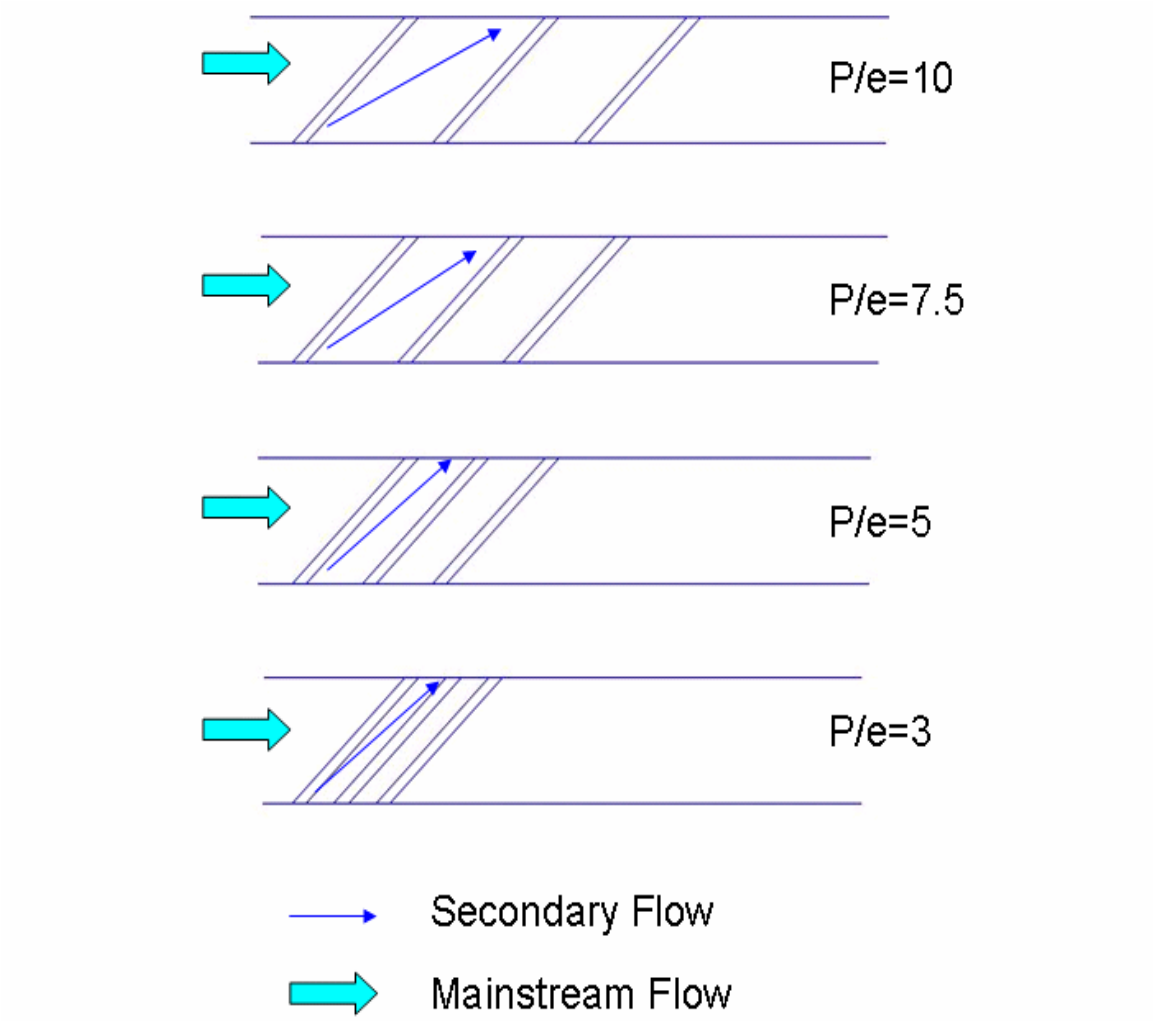

Fig. 3 Secondary Flow Behavior Induced by the 45° Angled Ribs

Effects of Rotation

The flow behavior for the 45° angled ribs under stationary condition is shown in Figure 4. The flow will be deflected an angle by the ribs. The flow will go toward the outer wall of the first pass and the inner wall of the second pass. The flow will be turnd at the turn region where the mixing of the secondary flow is strong. However, the Coriolis force and the rotational buoyancy force induced by rotation will strongly affect the heat transfer. The ribbed surface will cause flow separation and increase the turbulence in the boundary layer. The secondary flow generated by the rotation will redistribute the coolant in the channel and enhance the heat transfer. The effects of rotation with channel orientation at 90° are shown in Figure 4. The effect of rotation will result in higher heat transfer coefficients on the trailing surface in the first pass, while it is opposite in the second pass. Taslim et al. [8] used a liquid crystal technique to measure the heat transfer coefficient in a rotating channel with two opposite rib-roughened walls. Those were 90° angled ribs in the staggered arrangement. Three e/D_h ratios they tested are 0.1333, 0.25, and 0.333 for the Reynolds numbers ranging from 15000 to 50000. They concluded that compared to the stationary case, a maximum increase of about 45% in the heat transfer coefficient for the blockage ratio of 0.1333 and the minimum is a decrease of about 6% for the blockage ratio of 0.333.

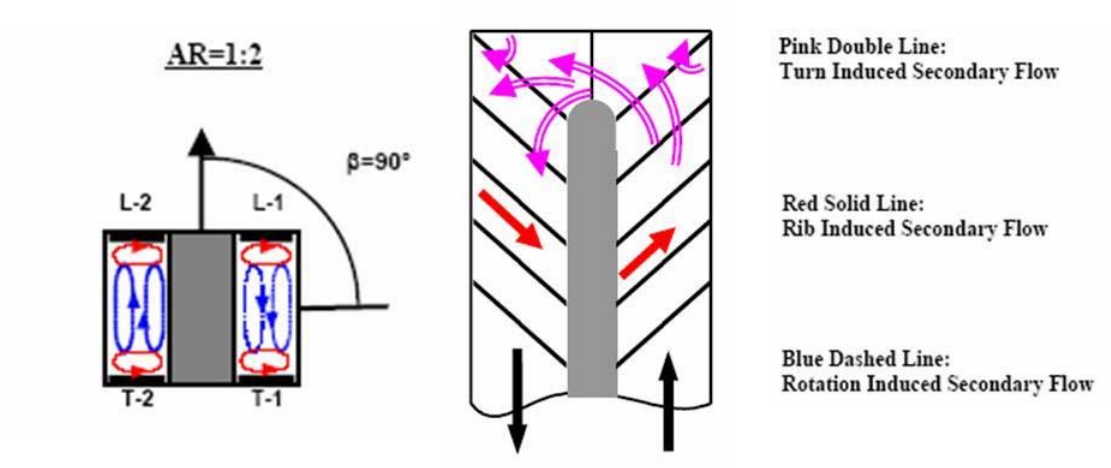

Fig. 4 Conceptual View of the Mainstream Flow and the Secondary Flow for the 45° Angled Ribs

Taslim et al. [9] investigated 45° criss-cross ribs on two opposite rib-roughened walls under stationary and rotating cases. The blockage ratios they studied are 0.1333, 0.25, and 0.3333 in the channels with aspect ratios of 1 and 2. The results show that for the high aspect ratio and the low blockage ratio, there is a steady increase in heat transfer coefficient on the trailing side as the rotating number increases. A steady decrease in heat transfer coefficient on the leading side with the rotation number is observed. The interaction of the secondary flow induced by rotation and the rib turbulators results in different heat transfer trends in the stationary and rotating cooling channels. This interaction is further complicated by varying the angle of attack of the ribs. Fu et al. [10] studied the heat transfer coefficients in two pass rectangular (AR=1:2 and 1:4) channels with 45° angled ribs. The non-rotating case is also tested as a comparison to the rotating case.

The objective of this research is to investigate the effect of rib spacing on the thermal performance of ribbed cooling channels with an aspect ratio of 1:2. The thermal performance is obtained by measuring the regionally averaged heat transfer coefficients and the overall pressure drop in the stationary and rotating channels. The spacing of the 45° angled ribs is varied so the spacing to height ratio (P/e) includes 3, 5, 7.5, and 10.

TEST FACILITY

The experiment will be tested in the facility that was used by Fu et al. [11], and can be seen in Figure 5. The test rig is composed of a rotating arm and a test section. The 1:2 test section is 12.7 x 25.4 mm in cross section. There is a 222.25 mm unheated entrance length in the test section to create a hydrodynamically fully developed flow condition. The cross section of the test section can be seen in Figure 6. It is composed of 4 parts: the leading wall, the trailing wall, the inner wall and the outer wall. Flexible heaters are put inside the Nylon substrate of the test section. Thermal conducting paste is used in the place between the copper plate and the heater to increase the thermal conductivity. The whole test section will be heated by the heaters for a period of time until the steady state is reached.

The copper plates are divided by the Nylon divider and silicon is used to seal the gap between each copper plate. Epoxy with high thermal conductivity has been used to glue the thermocouple in the 1.59 mm blind hole of each copper plate with 3.18 mm thickness. Those thermocouples are connected through a slip ring to a computer with a Labview System which can obtain the temperature measured by the thermocouples. The power supplied by the heater will be controlled to maintain the maximum wall temperature around 65°C.

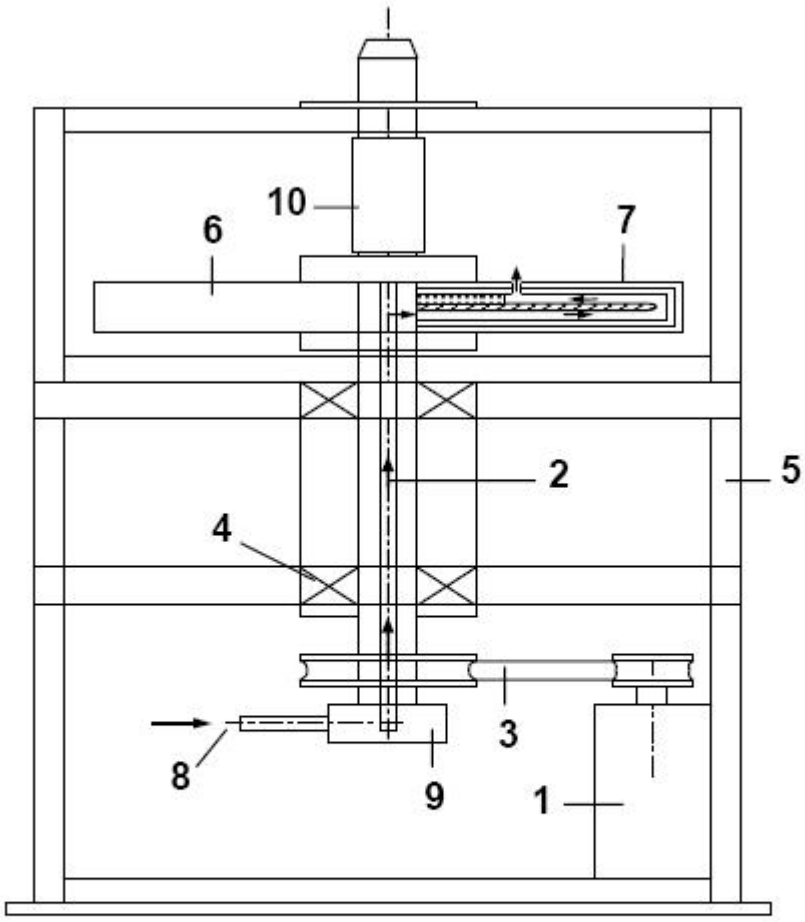

1. Electrical Motor with Controller
2. Rotating Shaft
3. Belt Drive Pulley System
4. Bearing Support System
5. Steel Table
6. Rotating Arm
7. Test Section
8. Compressor Air
9. Rotary Seal
10. Slip Ring

Fig. 5 Schematic of the Test Facility

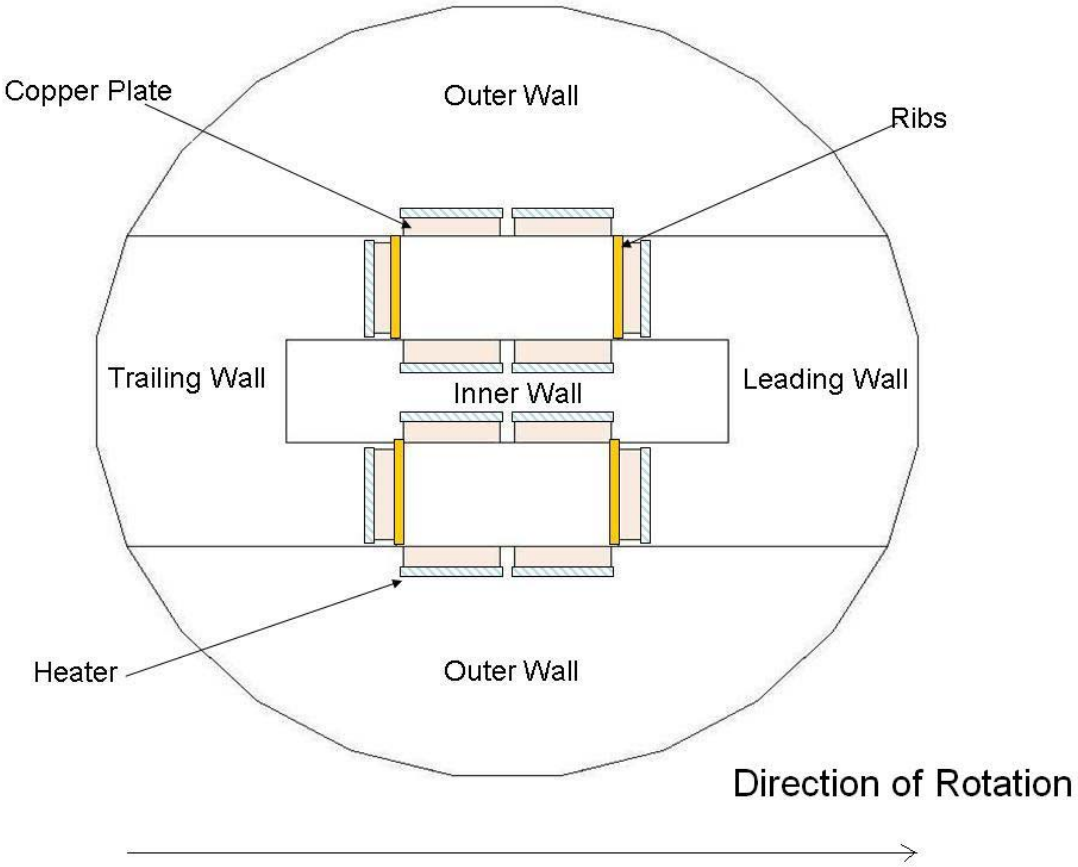

Fig. 6 Cross Sectional View of the Test Section with AR=1:2

The ribs are made of brass with 1.59 x 1.59 mm cross section. Super glue is used to glue the ribs on the leading wall and the trailing wall as shown in Figure 7. The super glue layer is very thin so the conduction between the rib and the copper plate is negligible. In order to maintain the same surface roughness of the ribs, sand paper is used to polish those ribs before putting them onto the copper plate before each test. The rib distributions are shown in Figure 8.

Static pressure taps are used to measure the pressure at the inlet and the outlet of the test section. Each pressure tap is connected to a separate channel of the Scani-Valve pressure transducer. Four pressure taps are used to measure the pressure; two are placed at the inlet and two are placed at the outlet of the test section. All four pressure taps are located on the outer walls of the test section. Manometer is used to calibrate the pressure measured by the pressure tap. The voltage signal obtained from the Scani-valve gives the gauge pressure of the test section at the inlet and the outlet.

A motor under the test rig is used to supply power to rotate the test rig clockwise or counterclockwise. A frequency controller is connected to the motor to control the rotation speed of the test rig. The rotating speed is fixed at 550rpm. The rotating number is approximately between 0.062-0.2. The rotating arm is a hollow cylinder made of aluminum and the test section is inserted into it. The channel orientation, β, is 90°with respect to the direction of rotation.

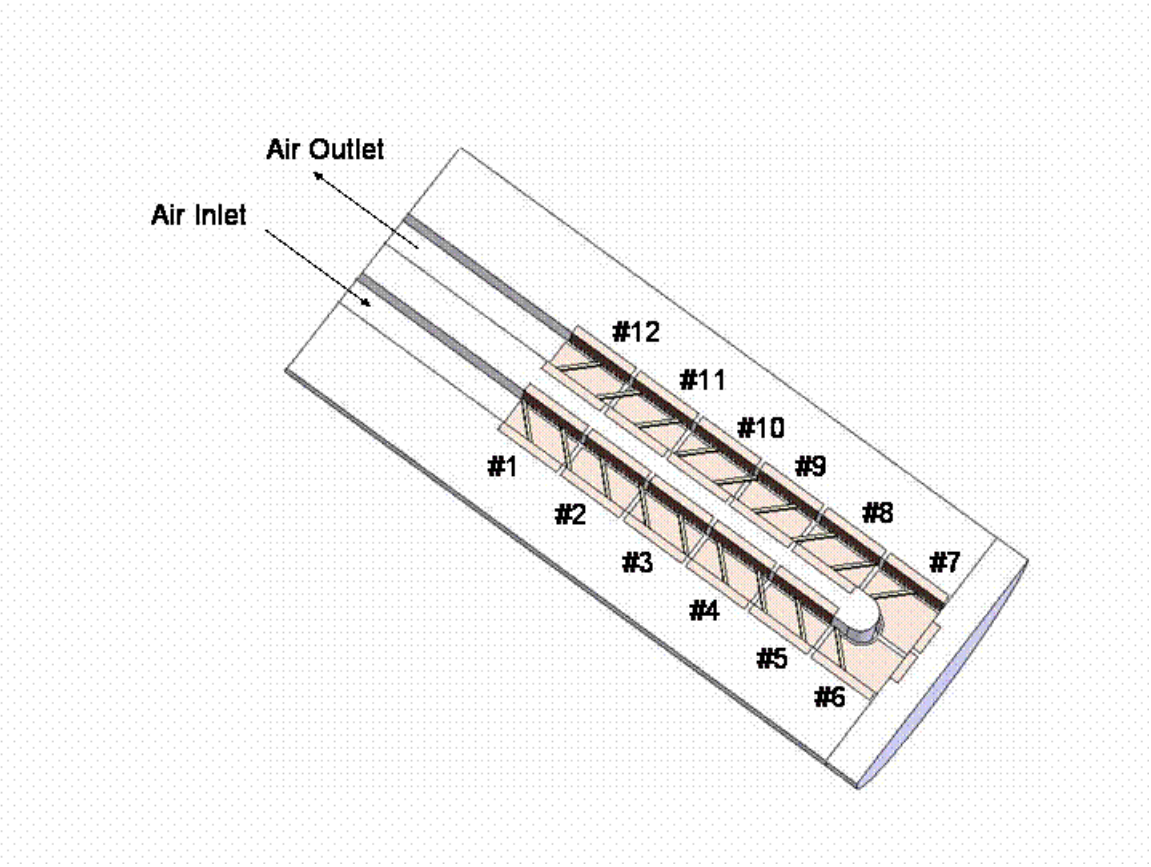

Fig. 7 Test Section with Ribs Attached to the Leading and Trailing Surfaces

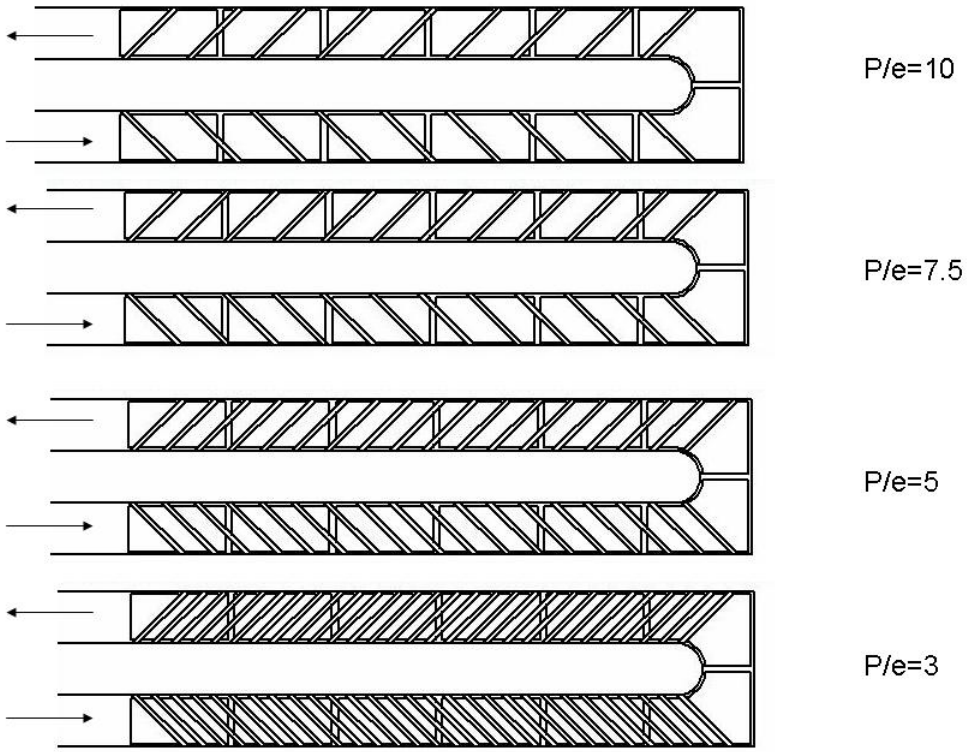

Fig. 8 Different Rib Distributions with the Mainstream Flow Direction

An ASME Orifice Flowmeter is used to control the mass flow rate of the cooling air. The Reynolds numbers are controlled at 5000, 10000, 25000 and 40000 by the corresponding mass flow rate. Because the rotational speed is fixed at 550 RPM, the rotational number is inversely proportional to the Reynolds number (mainstream coolant velocity). Table 1 shows the Reynolds numbers and the corresponding Rotation numbers.

Table 1 Reynolds Numbers and the Corresponding Rotation Numbers in the AR=1:2 Channel

Reynolds Number (Re)	Rotation Number (Ro)
5000	0.2101
10000	0.105
25000	0.042
40000	0.026

DATA REDUCTION

Heat Transfer Measurement

The purpose of the research is to investigate on the regionally averaged heat transfer coefficient in the rectangular channel with rib-roughened surface. By measuring the temperature of each copper plate and the energy supplied by the heater, we can get the regionally averaged heat transfer coefficient of each copper plate. The regional heat transfer coefficient can be calculated from:

$$h = \frac{q_w'' - q_{loss}''}{T_w - T_b} \qquad (1)$$

T_w is the wall temperature measured by the thermocouple and T_b is the bulk temperature calculated from linear interpolation between the inlet temperature and the outlet temperature. The heat flux from the heater q_w'' is calculated from the product of the heater voltage and current ($V \times I$). The heat loss will come from conduction through the wall. The heat losses are determined under a no flow condition, with fiberglass insulation in the channel to prevent natural convection between the walls.

The heat flux is calculated based on the area of the copper plate (A_{smooth}) and the area of the copper plate and the ribs (A_{total}). The heat transfer coefficients based on the two areas are also obtained and discussed. The ratios of the area increase by the ribs are shown in Table 2.

Table 2 Ratios of the Area Increase by the Ribs in the Channel

P/e	Area increased
10	26.47%
7.5	35.29%
5	52.94%
3	88.24%

From h, we can get the Nusselt number. The Dittus-Boelter/McAdams correlation is used to calculate the Nusselt number for the fully developed turbulent flow through a smooth stationary smooth circular tube. The Nusselt number ratio $\frac{Nu}{Nu_0}$ can be obtained:

$$\frac{Nu}{Nu_0} = \frac{hD_h}{k} \frac{1}{0.023\,\mathrm{Re}^{0.8}\,\mathrm{Pr}^{0.4}} \qquad (2)$$

All air properties are taken based on the bulk air temperature with a Prandtl number for air of 0.71.

Friction Factor Measurement

In order to measure the friction factor, the pressure difference between the inlet and the outlet must be obtained. The friction factor can be calculated from the pressure drop between the inlet and the outlet of the channel.

$$f = \frac{P_i - P_o}{4\left(\frac{L}{D_h}\right)\frac{1}{2}\rho U_m{}^2} \quad (3)$$

For the fully-developed friction factor in non-rotating smooth tube:

$$f_0 = 0.079\,\mathrm{Re}^{-0.25} \quad (4)$$

The friction factor ratio can be calculated by:

$$f / f_0 = f / 0.079\,\mathrm{Re}^{-0.25} \quad (5)$$

Thermal Performance

The thermal performance can show the combined effect of the heat transfer enhancement and the pressure drop penalty. The thermal performance is based on the following equation from Han et al [12]:

$$\eta = (Nu / Nu_0) / (f / f_0)^{1/3} \quad (6)$$

An uncertainty analysis is performed based on the method from Kline and McClintock [13]. The uncertainty from the thermocouple is about 0.5°C. The uncertainty for the heat transfer measurement is approximately 7% for the highest Reynolds number and the maximum is approximately 21% from the low heat flux wall for the lowest Reynolds number under rotating condition. The maximum uncertainty for the pressure measurement is 7% at Re=10000 and drops to 3% at Re=40000.

RESULTS AND DISCUSSION

Heat Transfer in Stationary Channels

The heat transfer coefficient for the P/e=10 case is shown in Figure 9. As the Reynolds number increases, the heat transfer effect will be enhanced due to high turbulent flow mixing. But the increasing Reynolds number will result in lower Nusselt number ratio. The results on the leading surface and the trailing surface are very close to each other due to symmetry geometry of the channel and the rib arrangements. There will be an enhancement in heat transfer in the turn region because of the strong secondary flow due to the structure of the turn. The dashed line is based on the smooth area and the solid line is based on the total area. The area difference between the smooth area and the total area for P/e=10 is 26.47%. The results based on the smooth area are higher than the total area because the area is smaller.

For the case of P/e=7.5 shown in Figure 10, heat transfer is promoted by the more flow reattachment phenomena caused by the ribs. The heat transfer coefficient is higher for P/e=7.5 compared to P/e=10. For the case of P/e=5 shown in Figure 11, there are more flow reattachment effects that will enhance the heat transfer more obviously. The result shows that the heat transfer coefficient is larger than the P/e=10 and P/e=7.5. For the 90° angled ribs, there will be a best heat transfer performance for P/e about 8. The flow will be tripped by those ribs and then reattach the surface .

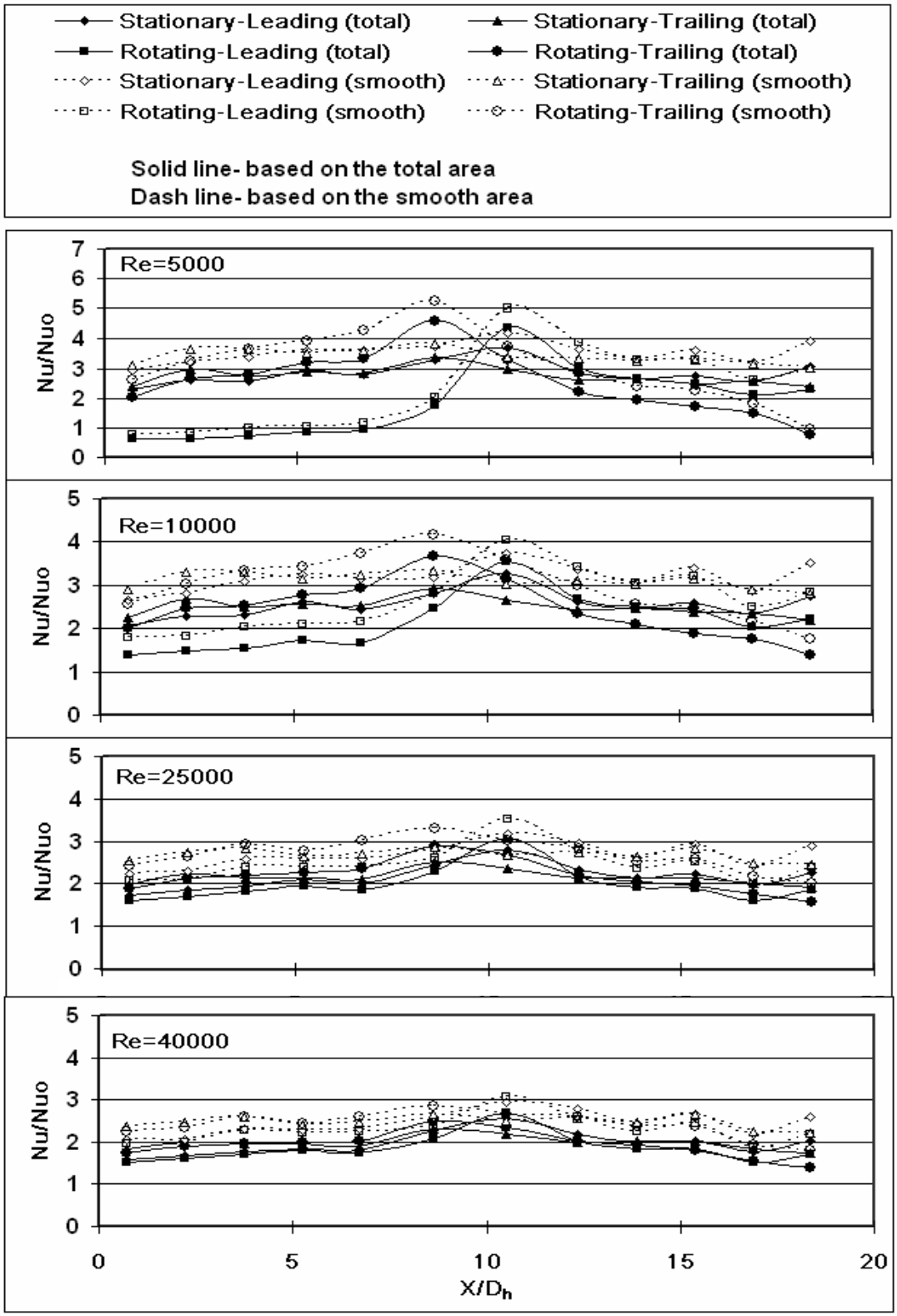

Fig. 9 Nusselt Number Ratio in the AR=1:2 Channel with P/e=10

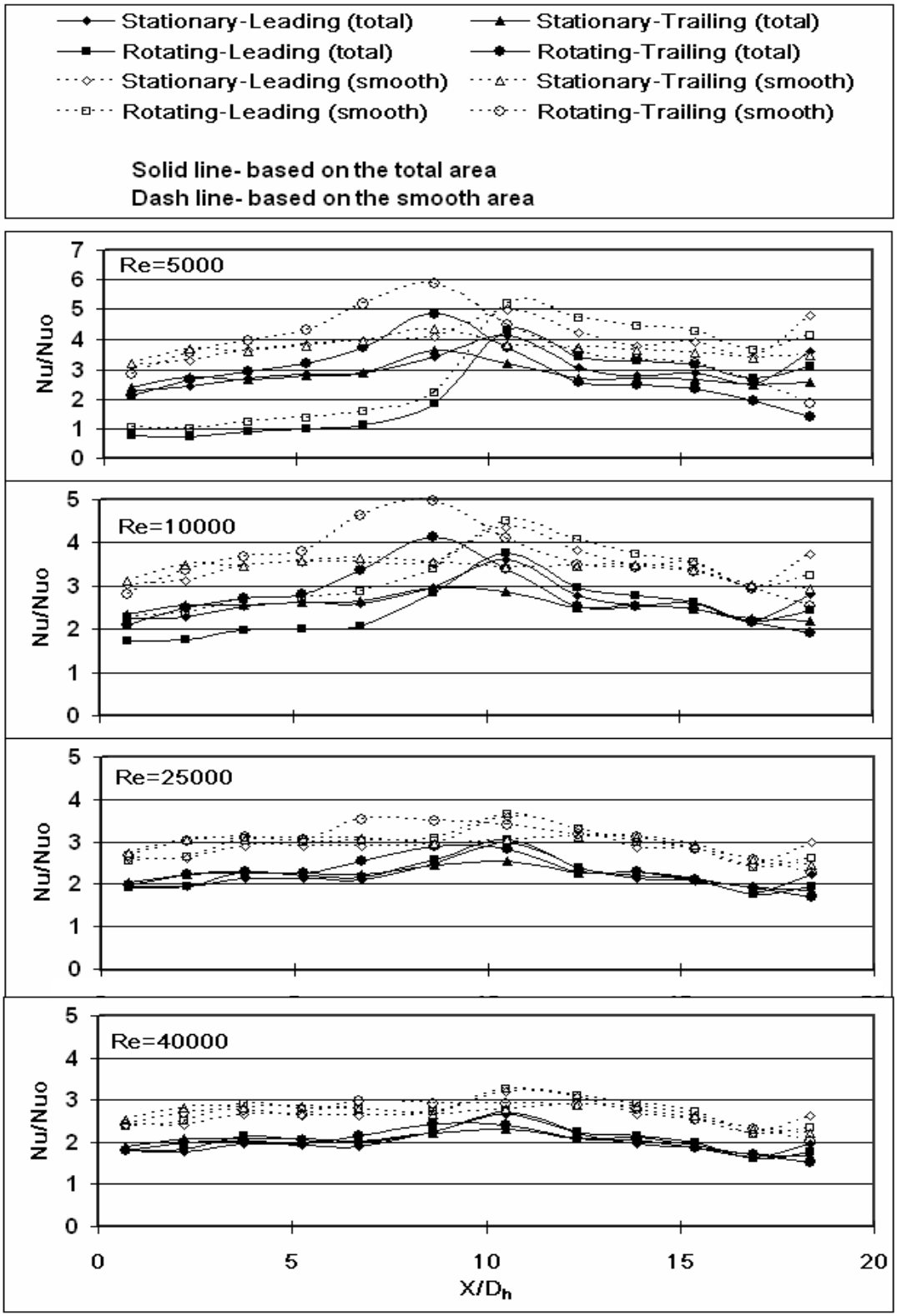

Fig. 10 Nusselt Number Ratio in the AR=1:2 Channel with P/e=7.5

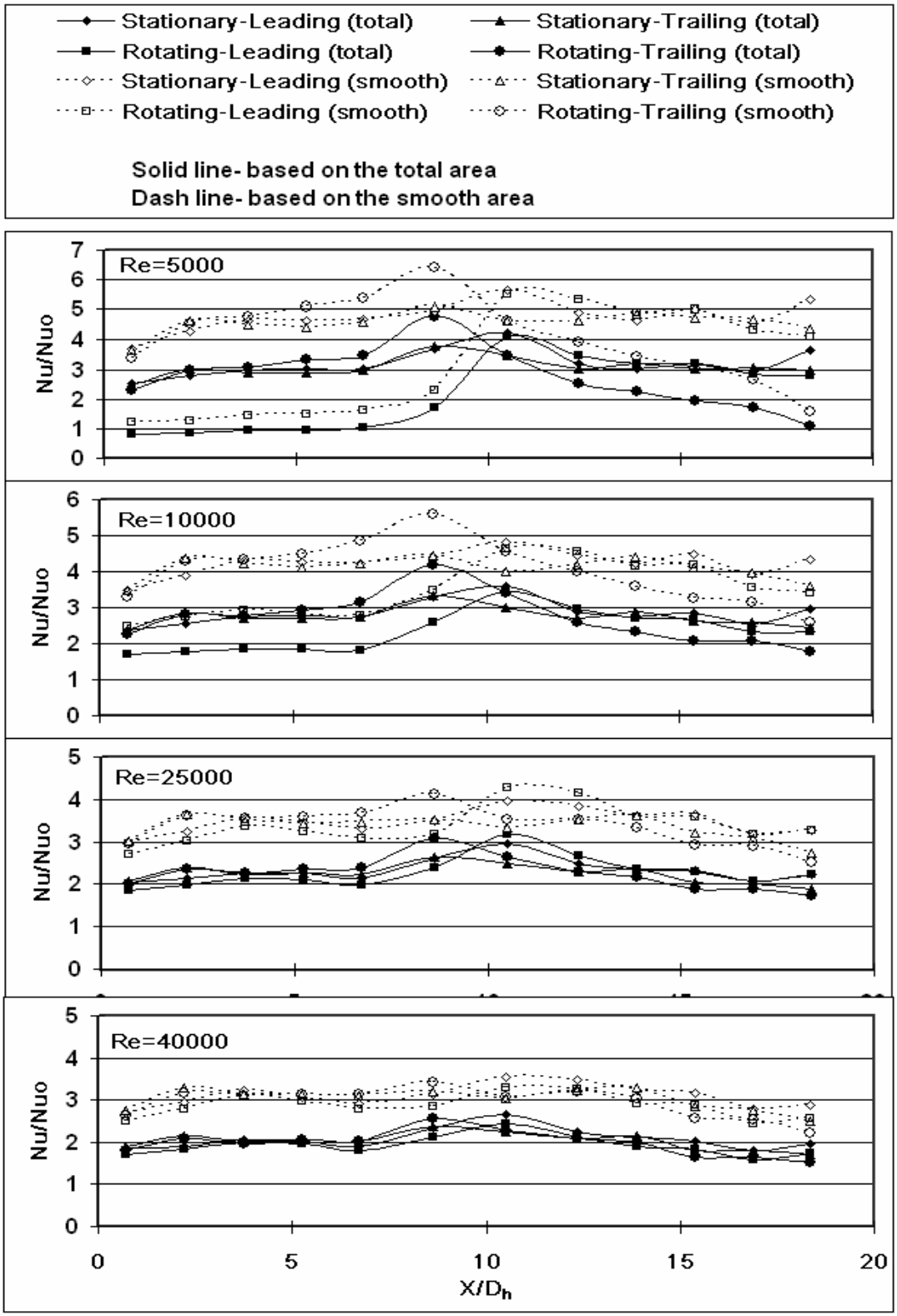

Fig. 11 Nusselt Number Ratio in the AR=1:2 Channel with P/e=5

The mainstream flow direction is normal to the ribs and enough space is needed for the flow to reattach the surface. But for the 45° angled ribs, the flow is deflected by the ribs and the secondary flow is created. The secondary flow developed along the angled-rib orientation will reattachment the surface more easily than the 90° angled ribs.

If the P/e ratio is too large, the flow will create a boundary layer after reattachment which will decrease the heat transfer coefficient, while if the distance between the ribs is too small, the flow will not reattach the surface due to the small distance. For the case of P/e=3 shown in the Figure 12, heat transfer coefficient is smaller compared to the other cases. The spacing between the ribs is too small that the flow will reach the next rib without reattaching the surface. Under this situation, the Nusselt number ratio will increase and the decrease as the Reynolds number increases.

The average heat transfer coefficients for the four cases are shown in Figure 13 and Figure 14. The heat transfer coefficients on the leading surface and the trailing surface are very close to each other. The results show that the greatest heat transfer enhancement occurs with P/e=5 for all four Reynolds numbers. The vortices induced by the ribs will impinge on the outer wall in the first pass and the inner wall in the second pass. For this reason, heat transfer enhancement is expected on the outer wall in the first pass and the inner wall in the second pass. The data is very close to the data from Fu et al. [11] in stationary channel.

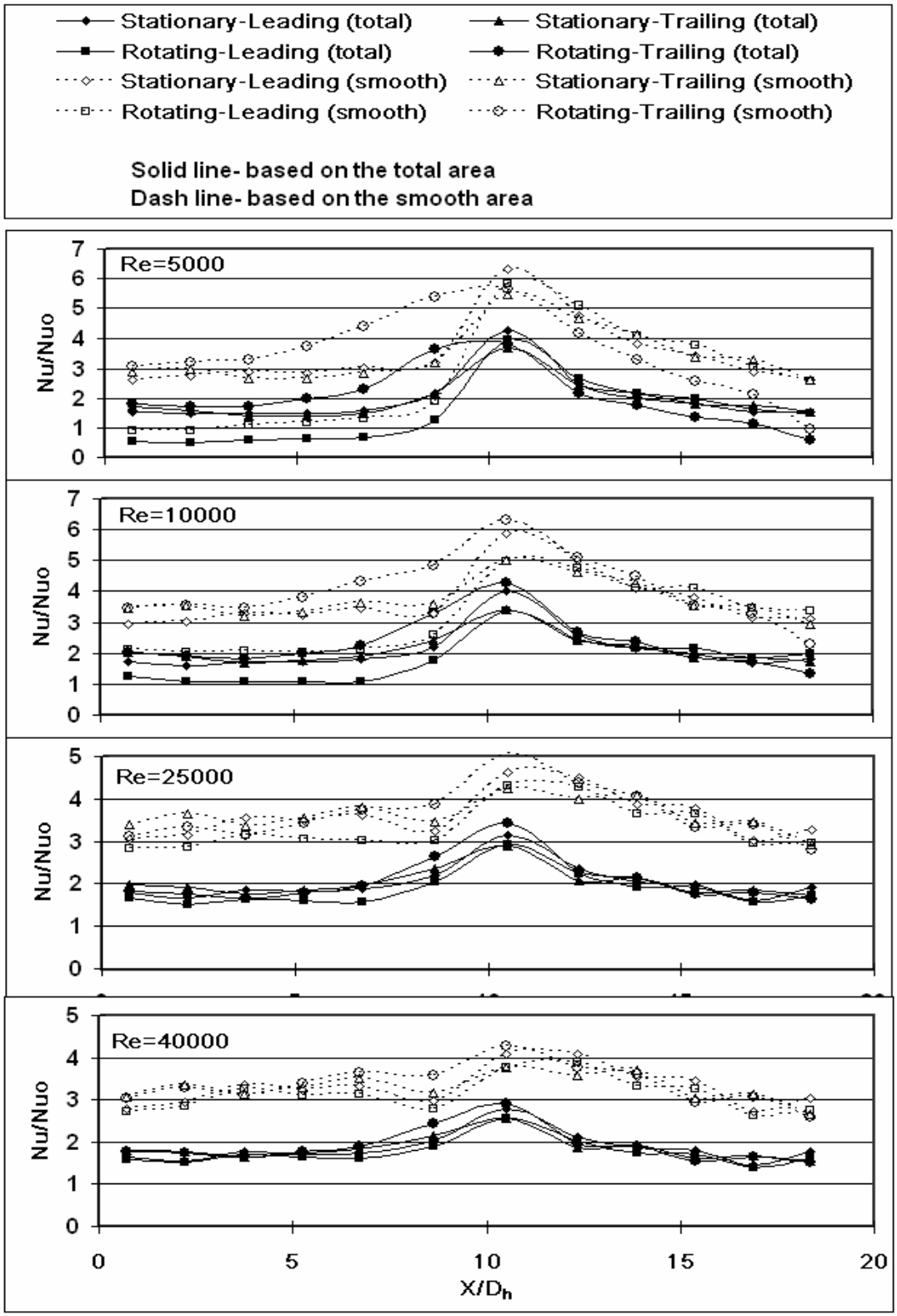

Fig. 12 Nusselt Number Ratio in the AR=1:2 Channel with P/e=3

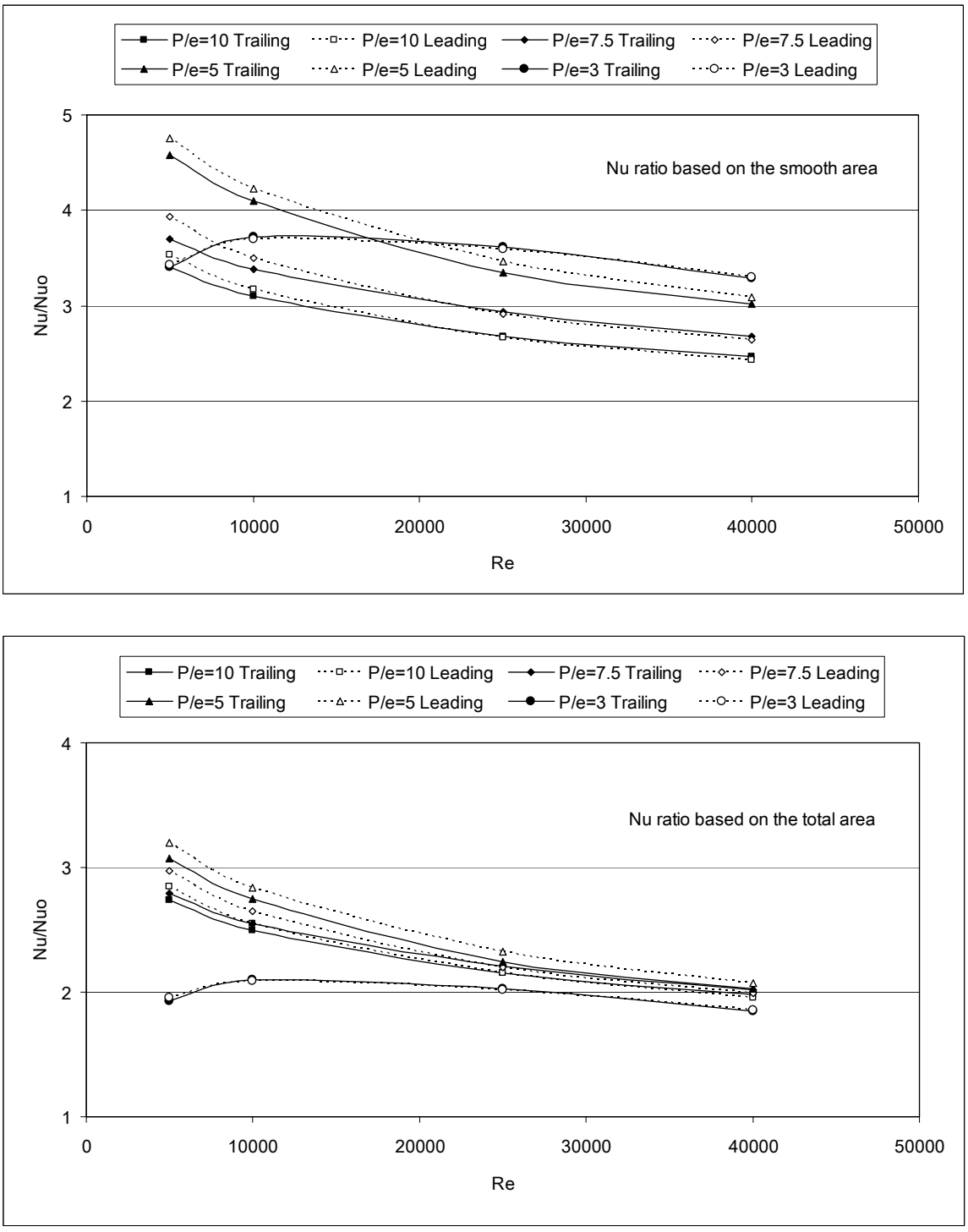

Fig. 13 Average Nusselt Number Ratios on the Trailing Surface and the Leading Surface for the Stationary Case

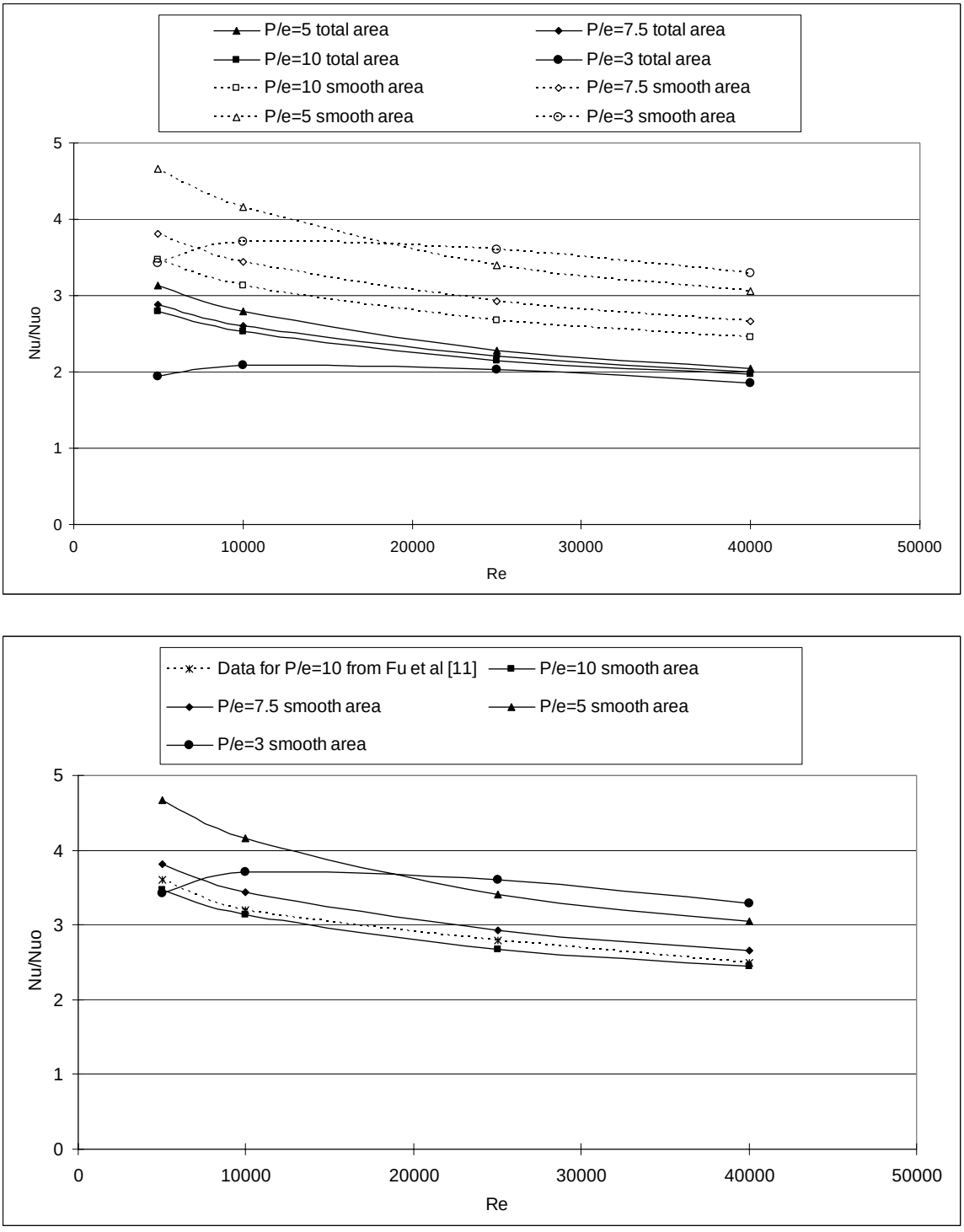

Fig. 14 Channel Average Nusselt Number Ratios for the Stationary Case

Heat Transfer in Rotating Channels

The heat transfer coefficient for P/e=10 under the rotating condition can be seen in Figure 9**.** The figure shows that the heat transfer coefficient in the trailing surface is higher than the leading surface in the first pass, while the result is opposite in the second pass. This is due to the Coriolis force and the rotational buoyancy force, which will push the flow toward the trailing surface in the first pass and the leading surface in the second pass. The rotation effect will decrease as the Reynolds number increases. The turn effect is much stronger than the rotation effect. The effect of rotation is stronger in the first pass than the second pass.

The secondary flow effect of the Coriolis force is the formation of a pair of counter-rotating vortices which is shown in Figure 4. The strength of the Coriolis force is dependent on the rotation number as follows:

$$Ro = \frac{\Omega D_h}{V} \qquad (7)$$

The rotation number is affected by the rotational speed of the channel, channel geometry, and the flow speed of the coolant.

For the P/e=7.5 case in Figure 10, the heat transfer coefficient is higher than P/e=10. The smaller spacing between the ribs allows more secondary flow vortex to enhance the heat transfer. For the P/e=5 case in Figure 11, the heat transfer coefficient is very close to 7.5, which is different from the stationary case. The rotating effect is stronger than the effect of the P/e ratio. The secondary flow created by the ribs will interact with the rotation induced secondary flow and the interaction produces different

results than were seen in the stationary channel. The result for P/e=3 shows the lowest heat transfer coefficients in Figure 12. In this case, the spacing between the ribs is too small and there is not enough space for the flow to reattach the surface. The average Nusselt number ratios for the rotating cases are shown in Figure 15 and Figure 16**.** Because of the rotation effect, the heat transfer coefficients are higher in the trailing surface compared to the leading surface. The results show that the Nusselt number ratio will increase and then decrease as the Reynolds number increases. The highest heat transfer is between 7.5 and 5. Compared to the data from Fu et al. [11], the data is about 33% lower for Re=5000 case and 5% lower for the Re=40000 case. This may comes from the high uncertainty at the low Reynolds number, while the uncertainty decreases as the Reynolds number increases. The Nusselt number ratios with respect to the Rotation numbers are shown in Figure 17 and Figure 18. A higher Rotation number signifies more rotational effects on the flow and heat transfer. But the effect of the rotation is not significant. The heat transfer will increase on the trailing surface in the first pass and the leading surface in the second pass. This is due to two reasons: (1) the rotational effect will push the flow toward these respective surfaces, and (2) the flow is deflected by the ribs and secondary flow is generated toward these surfaces. The Nusselt Number ratios will increase with the rotation number.

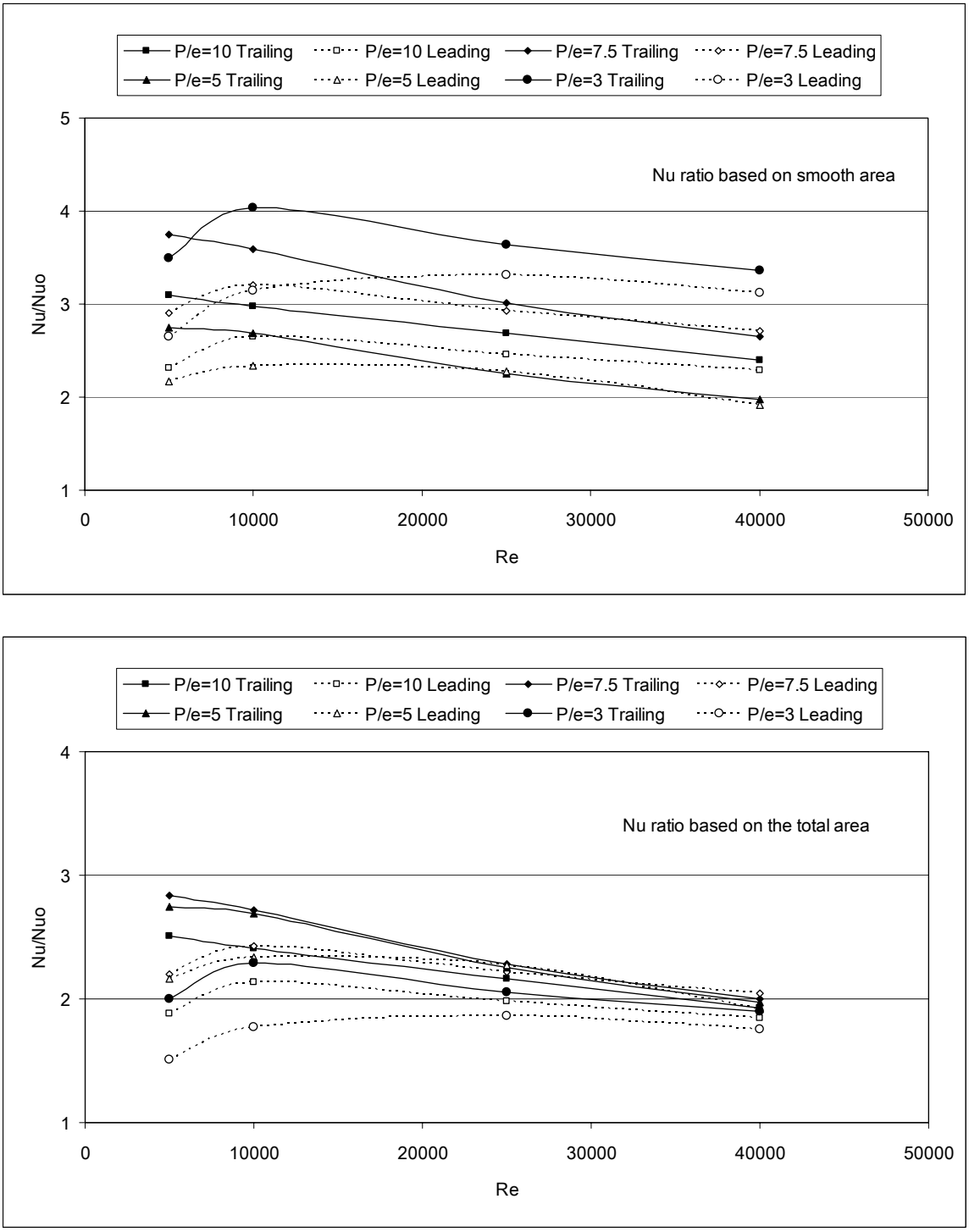

Fig. 15 Average Nusselt Number Ratios on the Trailing Surface and the Leading Surface for the Rotating Case

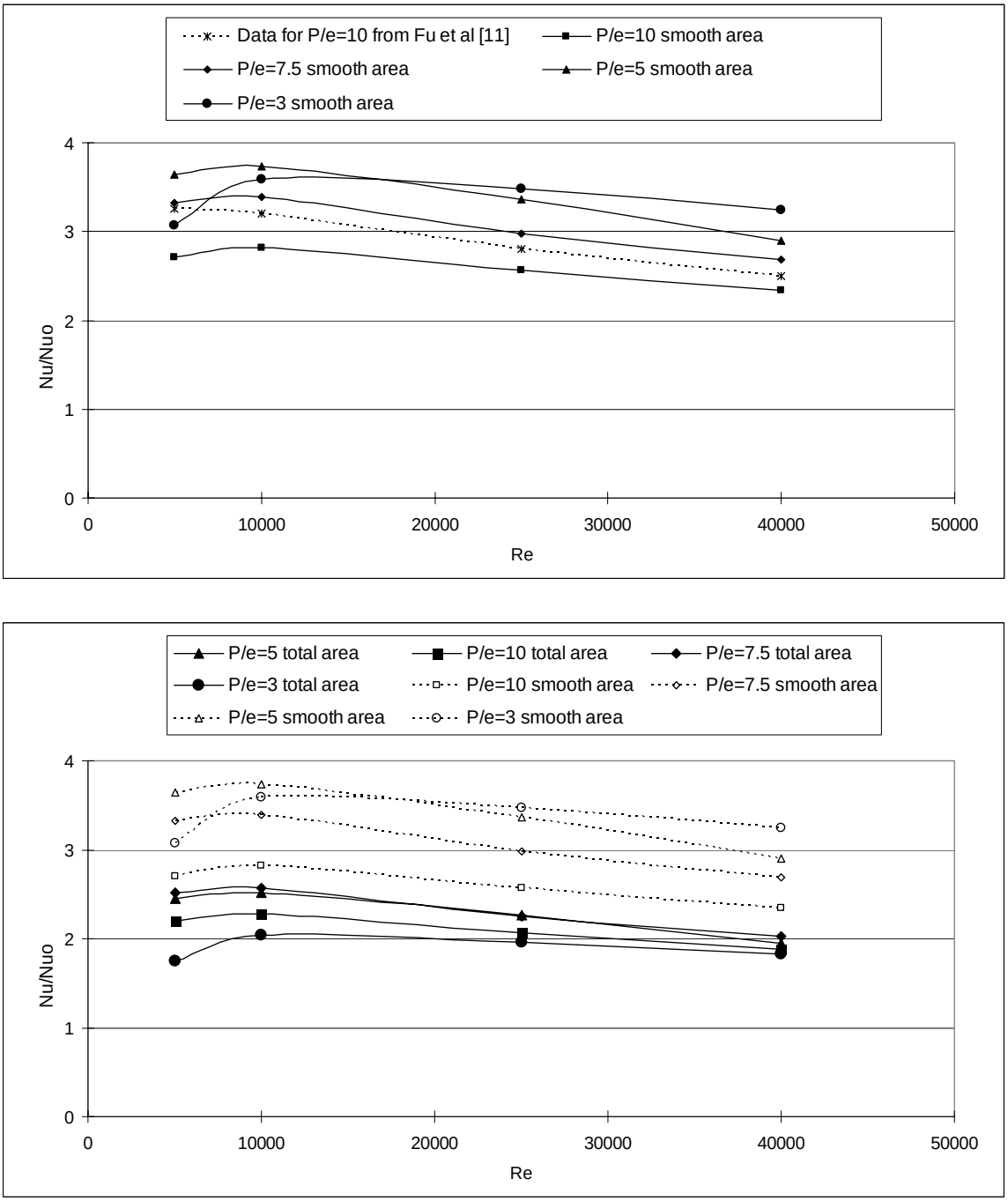

Fig. 16 Channel Average Nusselt Number Ratios for the Rotating Case

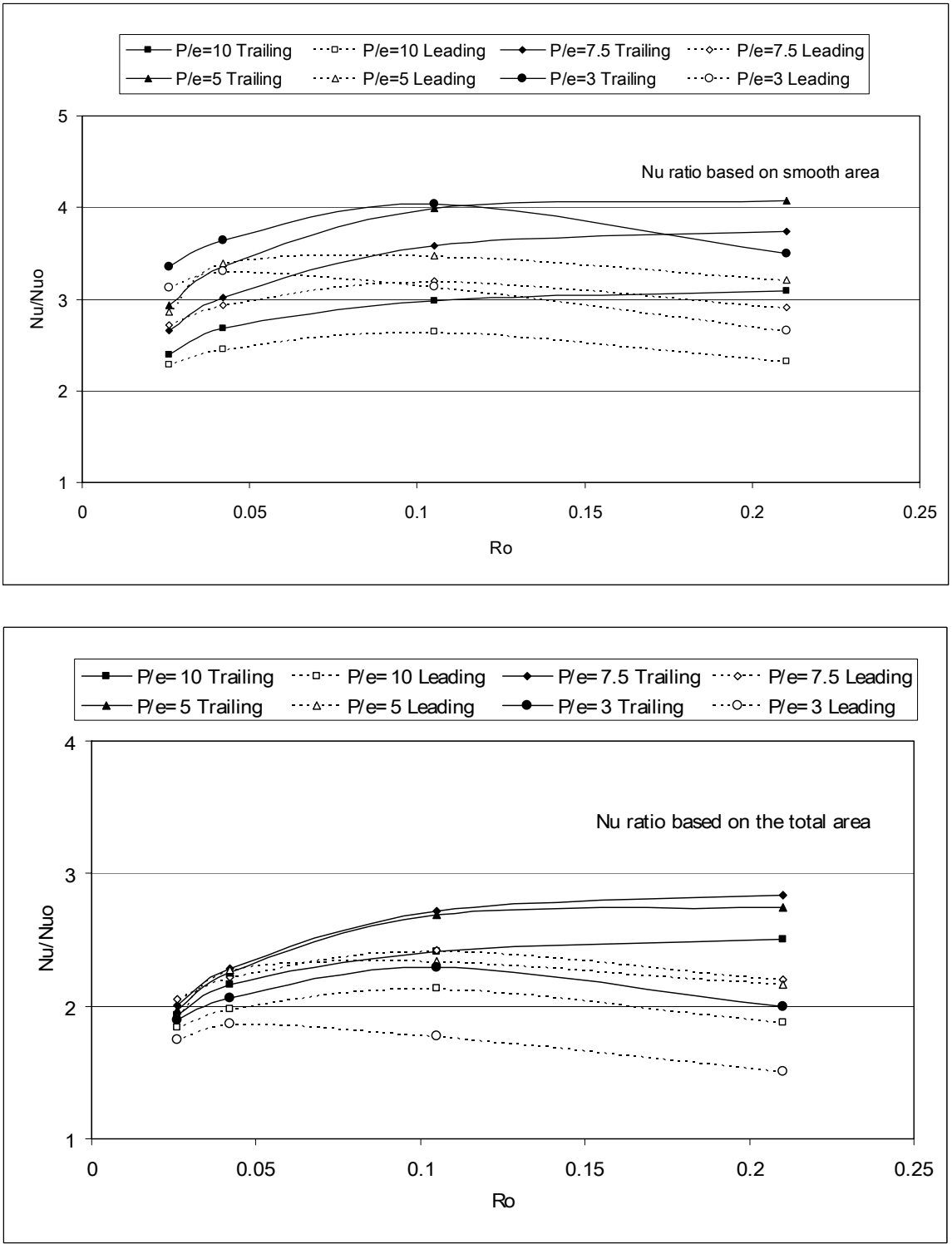

Fig. 17 Average Nusselt Number Ratios on the Trailing Surface and the Leading Surface for the Rotating Case Based on the Rotation Number

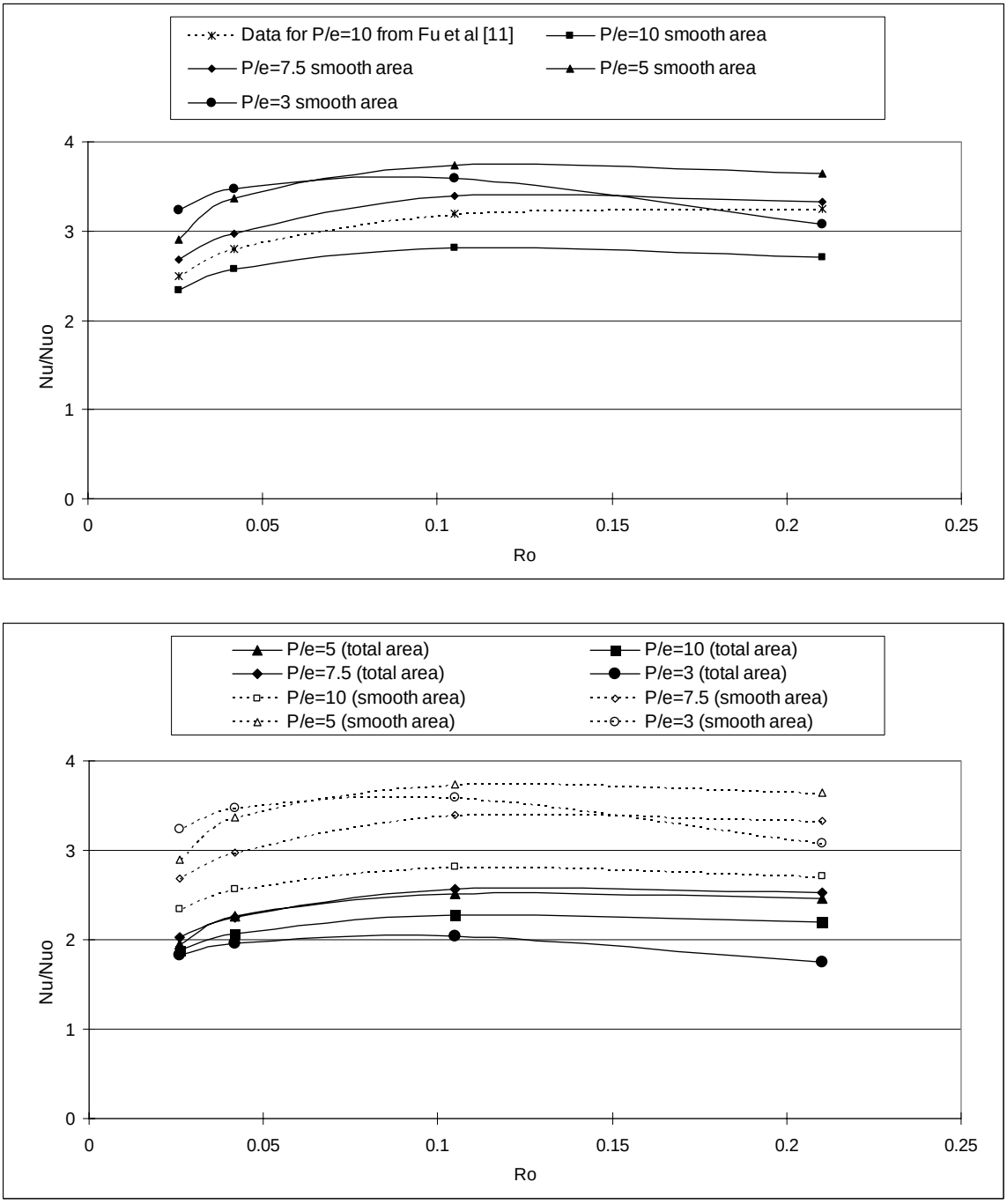

Fig. 18 Channel Averaged Nusselt Number Ratios for the Rotating Case Based on the Rotation Number

The buoyancy parameter is important due to high rotational speed and the large temperature difference. The rotational-induced buoyancy force aids the inertia force for the radial outward flow in the first pass. In the second pass, the buoyancy force will oppose the inertia force because the flow direction is reversed. A buoyancy parameter is used to represent the buoyancy force:

$$Bo_x = \left(\frac{\Delta\rho}{\rho}\right)_x Ro \frac{R_x}{D_h} \tag{8}$$

The local buoyancy parameter can be re-written by substituting the density ratio by the measured wall and coolant temperatures:

$$Bo_x = \frac{T_{w,x} - T_{b,x}}{T_{f,x}} Ro \frac{R_x}{D_h} \tag{9}$$

The local film temperature is the average of the local wall and the local coolant temperatures.

$$T_{f,x} = (T_{w,x} + T_{b,x})/2 \tag{10}$$

The buoyancy effects for the first pass and the second pass are shown in Figure 19 and Figure 20, respectively. The data is taken at the number 4 copper plate in the first pass and the number 11 copper plate in the second pass, as shown in Figure 7. The result in the first pass shows that the heat transfer increases with the buoyancy factor in the trailing surface and decrease with the buoyancy factor in the leading surface. This is because the rotation will push the coolant toward the trailing surface. In the second pass, the rotation will push the air in the leading surface and increase the heat transfer with the buoyancy factor.

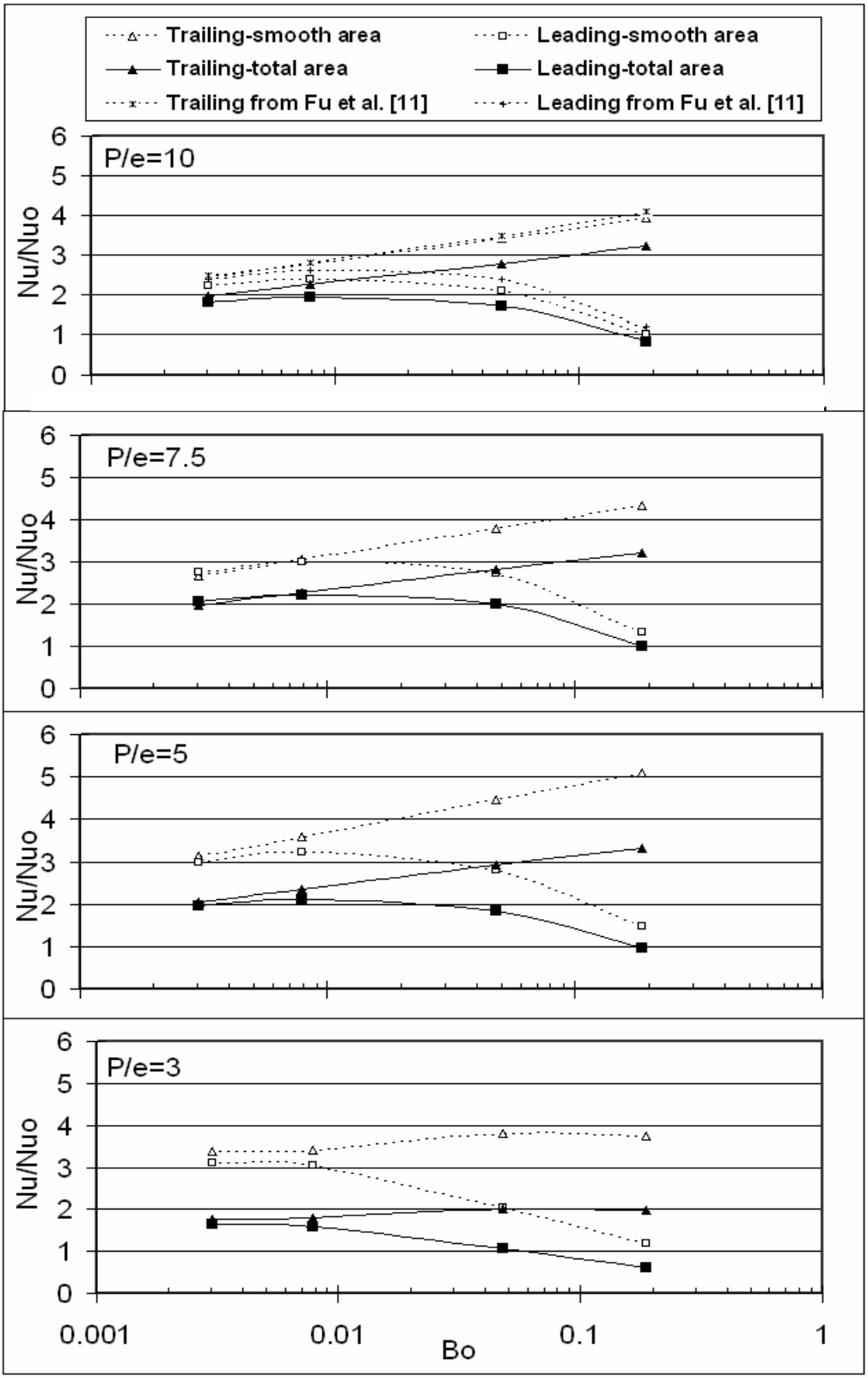

Fig. 19 Effect of the Buoyancy Factor on Heat Transfer in the First Pass

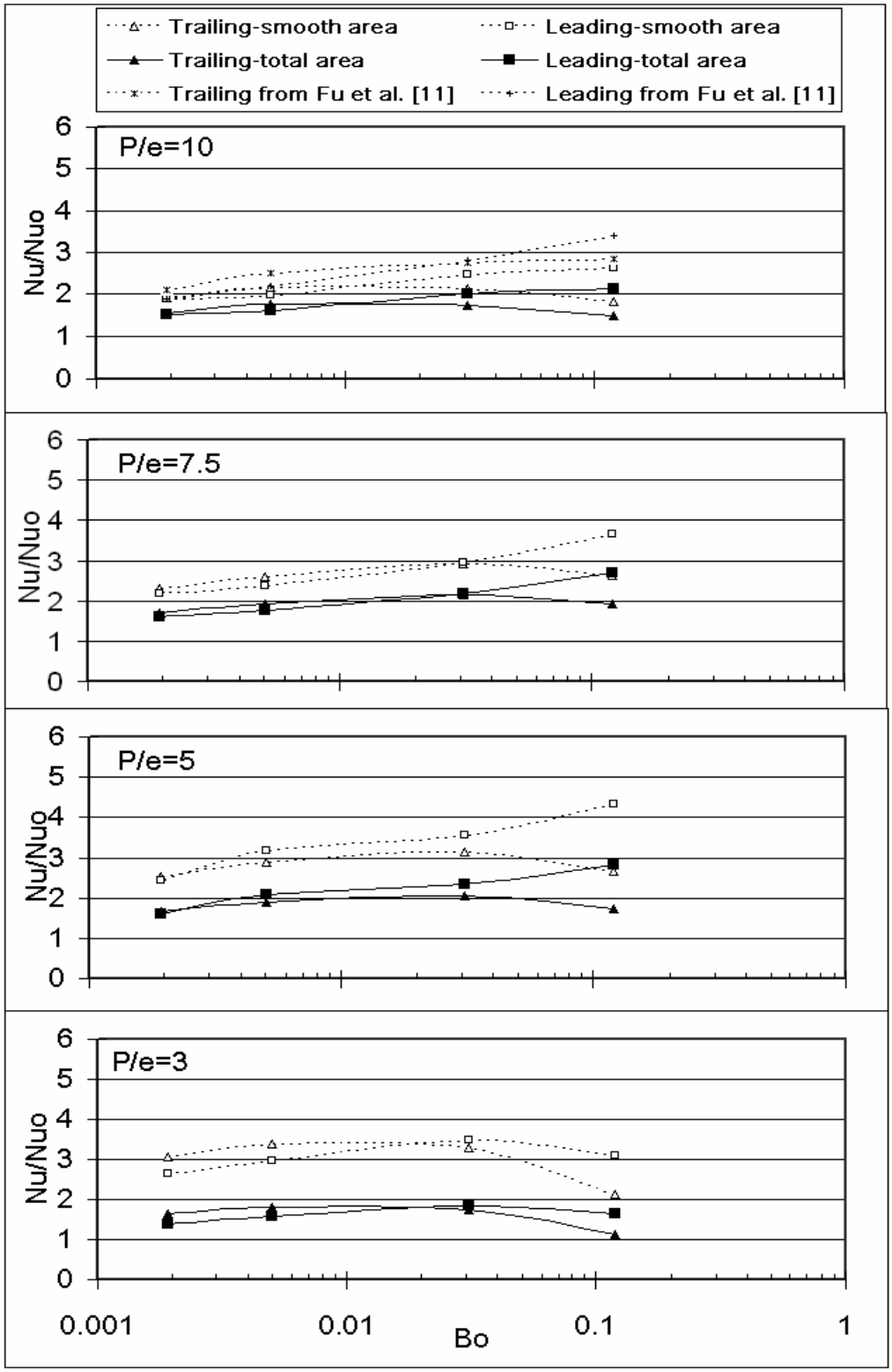

Fig. 20 Effect of the Buoyancy Factor on Heat Transfer in the Second Pass

Pressure Drop and Thermal Performance

The ribs will trip the flow and flow reattachment will occur. This increases the pressure drop through the ribbed channels. The result of the friction factor ratios for the stationary case is shown in Figure 21. The highest pressure drop is in the P/e=3 because the largely increasing number of the ribs. The P/e=10 case shows the lowest friction factor ratio, which has the fewest number of the ribs. The pressure drop for P/e=3 is about 30 % higher than P/e=10. The rotating data can also be seen in Figure 21**.** The pressure drop data from Fu et al. [11] is about 30% higher compared to the data for P/e=10 under rotation condition. The difference may come from the uncertainty. However, the data is between the experimental data and the CFD prediction. Again, more ribs block more air and result in higher pressure drop.

Finally, with the Nusselt number and the friction factor ratio, the thermal performance of each rib distribution can be obtained as shown in Figure 22 and Figure 23. The thermal performance from Fu et al [11] is higher because the heat transfer coefficient is calculated based on the smooth area of the copper plate. For the case of P/e=5, the thermal performance is a little higher than the cases of P/e=10 and 7.5 under stationary case. Because of the heat transfer is highest but with a high pressure drop penalty. For the rotating condition, the P/e=7.5 is the highest thermal performance due to the highest heat transfer.

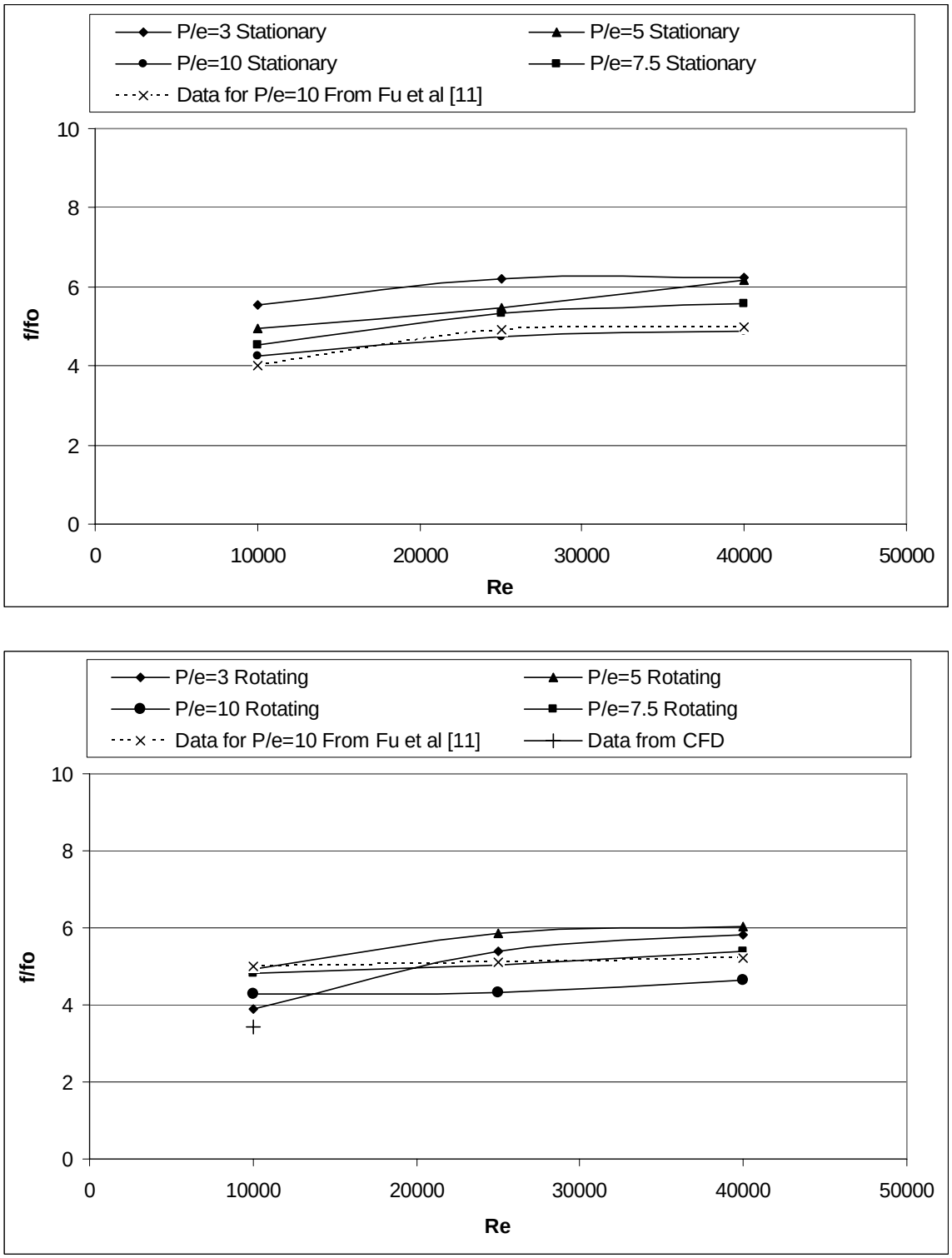

Fig. 21 Overall Friction Factor Ratios for the Stationary and the Rotation Cases

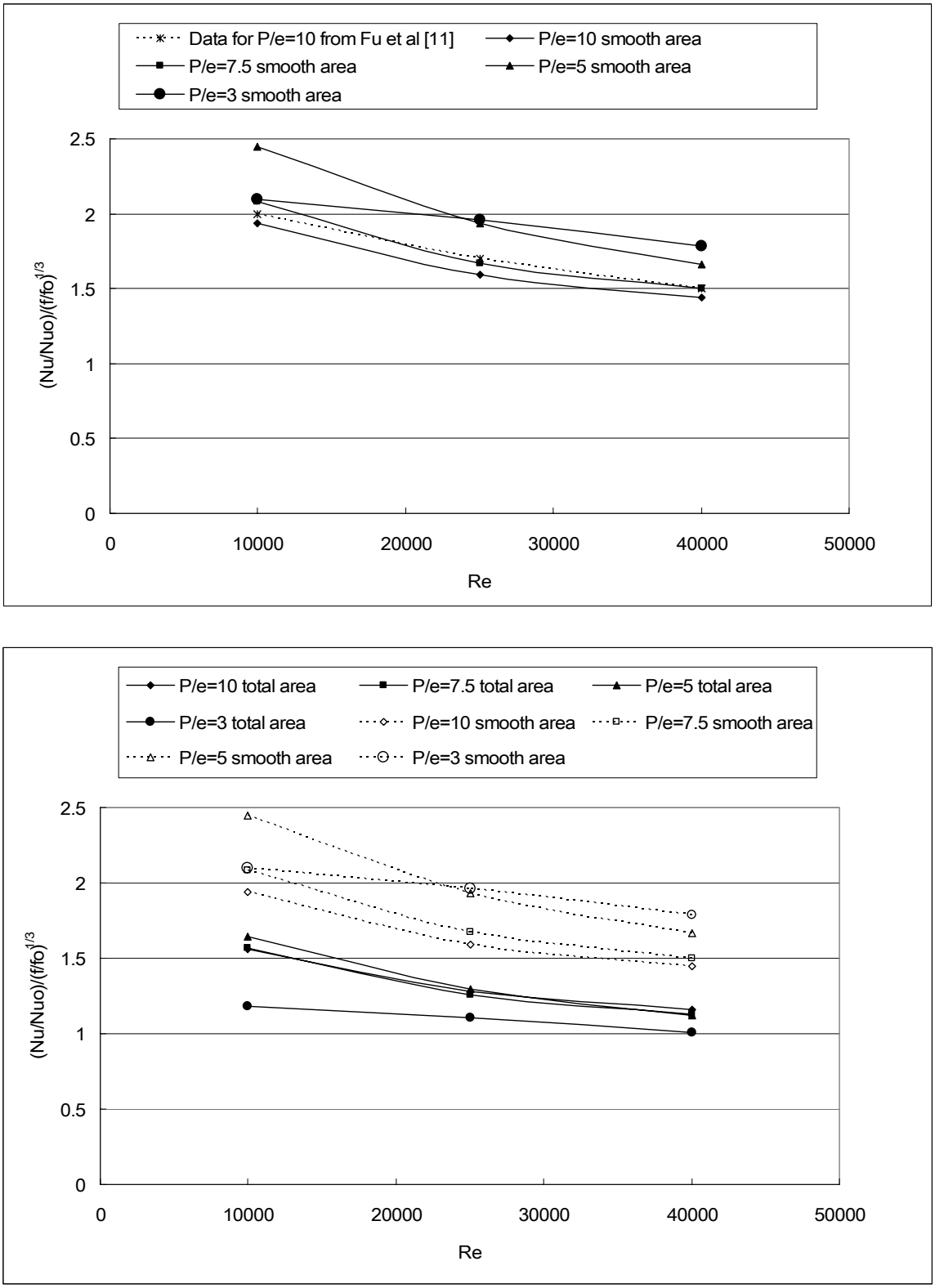

Fig. 22 Thermal Performances for the Stationary Cases

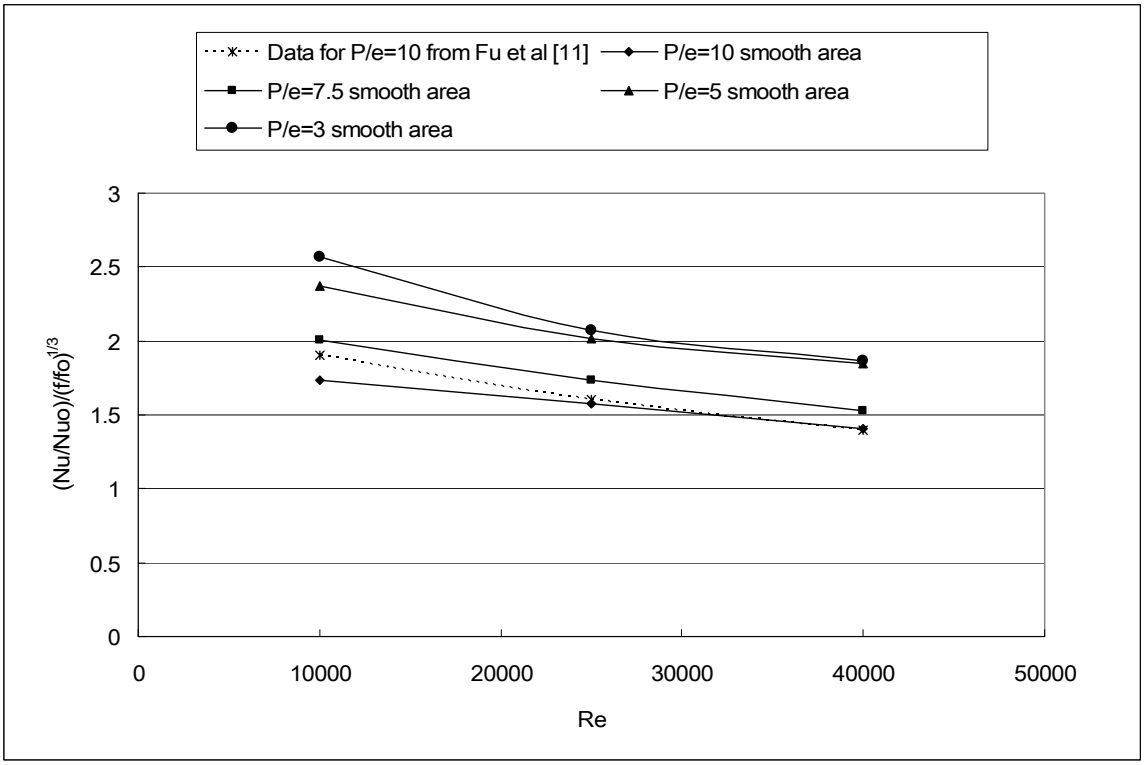

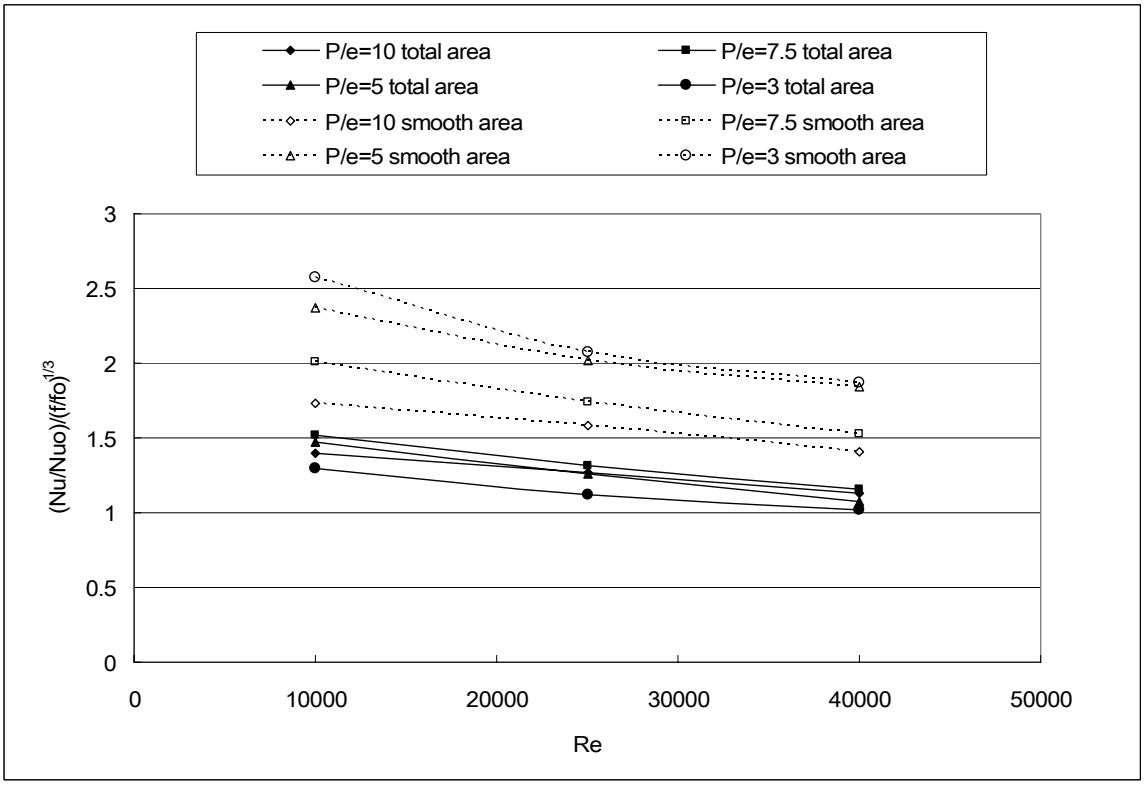

Fig. 23 Thermal Performances for the Rotating Cases

CONCLUSIONS

For the 45° angled ribs, the P/e =5 produces higher heat transfer coefficients than P/e=10, 7.5 and 3 in stationary channels, while the P/e between 5 and 7.5 will produce highest heat transfer coefficients in rotating channels. The rotation effect is strong at low Reynolds numbers and the effect decreases as the Reynolds number increases.

For the pressure drop, more ribs will trip more air and result in higher pressure drop. The friction factor ratio is the highest in the P/e=3 case and the lowest in the P/e=10 case under stationary condition. But under rotation condition, P/e=5 is the highest friction factor ratio and P/e=10 is the lowest .

The flow structure for the 45° angled ribs is different from the 90° angled ribs. The secondary flow direction is strongly affected by the angle of the flow attack. The highest thermal performance is between P/e=5 and P/e=7.5 under stationary case and about P/e=7.5 under rotating condition.

The results calculated based on the smooth area will obtain higher heat transfer coefficient as well as higher thermal performance. In actual engine design, this is not safe. The result calculated based on the total area can get smaller heat transfer coefficient and is more conservative and safer in actual engine design.

REFERENCES

[1] Han, J. C., Dutta, S., and Ekkad, S. V., 2000, *Gas Turbine Heat Transfer and Cooling Technology*, Taylor and Francis, New York.

[2] Taslim, M. E. and Lengkong, A., 1998, "45 deg Staggered Rib Heat Transfer Coefficient Measurements in a Square Channel," J. of Turbomachinery, **120**, pp. 571-580

[3] Taslim, M. E. and Korotky, G. J., 1998, "Low-Aspect-Ratio Rib Heat Transfer Coefficient Measurements in a Square Channel," J. of Turbomachinery, **120**, pp. 831-838

[4] Han, J. C., 1984, "Heat Transfer and Friction in Channels with Two Opposite Rib-Roughened Walls," J. of Heat Transfer, **106**, pp. 774-781

[5] Taslim, M. E. and Spring, S. D., "Effects of Turbulator Profile and Spacing on Heat Transfer and Friction in a Channel," J. of Thermophysics and Heat Transfer, **8**, No. 3, pp. 555-562

[6] Han, J. C., 1988, "Heat Transfer and Friction Factor Characteristics in Rectangular Channels with Rib Turbulators," J. of Heat Transfer, **110**, pp. 321-328

[7] Han, J. C., Glicksman L. R., and Rohsenow, W. M., 1978, "An Investigation of Heat Transfer and Friction Factor for Rib-Roughened Surfaces," Int. J. of Heat Mass Transfer, **21**, pp. 1143-1156

[8] Taslim, M. E., Rahman, A., Spring, S. D., "An Experimental Investigation of Heat Transfer Coefficients in a Spanwise Rotating Channel with Two Opposite Rib-Roughened Walls," J. of Turbomachinery, **113**, pp. 75-82

[9] Taslim, M. E., Bondi, L. A., Kercher, D. M., "An Experimental Inversigation of Heat Transfer in an Orthogonally Rotating Channel Roughened with 45 deg Criss-Cross Ribs on Two Opposite Walls," J. of Turbomachinery, **113**, pp. 346-353

[10] Fu, W. L., Wright, L. M., Han, J. C., 2005, "Heat Transfer in Two-Pass Rotating Rectangular Channels (AR=1:2 and AR=1:4) with 45° Angled Rib Turbulators," Journal of Turbomachinery, **127**, pp. 164-174

[11] Fu, W. L., Wright, L. M., Han, J. C., 2005, "Buoyancy Effects on Heat Transfer in Five Different Aspect-Ratio Rectangular Channels with Smooth Walls and 45-Degree Ribbed Walls," Paper No. GT 2005-68493, IGTI Turbo Expo, Reno, NV.

[12] Han, J. C., Park, J. S., and Lei, C. K., 1985, "Heat Transfer Enhancement in Channels with Turbulence Promoters," ASME Journal of Engineering for Gas Turbines and Power, **107**, pp. 628-635

[13] Kline, S. J. and McClintock, F. A., 1953, "Describing Uncertainty in Single-Sample Experiments," Mechanical Engineering, **75**, pp. 3-8

VITA

Yao-Hsien Liu was born in Taichung, Taiwan on the 27th day of May. He received his Bachelor of Science in mechanical engineering from National Taiwan University (NTU) in June 2002. He worked as a research assistant in the Micro-Mechanism Lab in the Department of Mechanical Engineering at NTU from November of 2002 to June of 2003. In September of 2003, he began his graduate studies in Texas A&M University.

While in graduate school at Texas A&M, he worked in the turbine heat transfer laboratory with Dr. J. C. Han. Upon completion of his Master of Science degree in mechanical engineering (August 2005), he plans to continue his study to earn a Ph.D. degree in Mechanical Engineering.

Mailing Address

Yao-Hsien Liu

101 Front Street 308

College Station, Texas, 77840